Supplementary Information for:

Optically-pure triptycene-based metallomacrocycles and homochiral self-sorting assisted by ladder formation

Kosuke Oki,[‡a] Wei Zheng,[‡a,b] Eiji Yashima[a] and Tomoyuki Ikai*[a,c]

[a] Department of Molecular and Macromolecular Chemistry, Graduate School of Engineering, Nagoya University, Chikusa-ku, Nagoya 464-8603, Japan

[b] Present address: College of Materials Science and Engineering, Tongji University, Shanghai, 201804, China

[c] Precursory Research for Embryonic Science and Technology (PRESTO), Japan Science and Technology Agency (JST), Kawaguchi, Saitama 332-0012, Japan

‡ These authors contributed equally to this work.

*Correspondence: ikai@chembio.nagoya-u.ac.jp

Table of Contents

1. Instruments and Materials

Instruments. The melting points were measured on a Yanako melting point (Yanako, Kyoto, Japan) and were uncorrected. The microwave-assisted Suzuki-Miyaura cross-coupling reaction was performed using an Anton Paar Monowave 400 reactor (Anton Paar, Graz, Austria). The NMR spectra were measured using a Varian 500AS (Agilent Technologies, Santa Clara, CA) or a Bruker Ascend 500 (Bruker Biospin, Billerica, MA) spectrometer operating at 500 MHz for ^{1}H, 126 MHz for ^{13}C, and 203 MHz for ^{31}P using tetramethylsilane (^{1}H and ^{13}C) and 85% H_3PO_4 in H_2O (^{31}P) as the internal and external standards, respectively. The IR spectra were recorded on a JASCO FT/IR-680 spectrophotometer (JASCO, Tokyo, Japan). The absorption and circular dichroism (CD) spectra were obtained in a 1.0-mm quartz cell using a JASCO V-750 spectrophotometer and a JASCO J-820 spectropolarimeter, respectively. The temperature was controlled with JASCO ETCS-900 and JASCO PLC-423L apparatuses for absorption and CD measurements, respectively. The photoluminescence (PL) and circularly polarized luminescence (CPL) spectra were recorded at 25 °C on a JASCO CPL-300 spectrophotometer with a 10-mm quartz cell. A scanning rate of 100 nm min^{-1}, an excitation slit width of 3000 μm, a monitoring slit width of 3000 μm, a response time of 4 seconds, and 32 times accumulations were employed for the CPL measurements. Fluorescence quantum yields were measured with a JASCO FP-8550 spectrofluorometer attached with a JASCO ILF-135 integrating sphere (diameter 120 mm). The high-resolution mass spectra (HRMS) were recorded on JEOL JMS-T100GCV (JEOL, Akishima, Japan), Thermo Fisher Scientific Exactive Plus (Thermo Fisher Scientific, Waltham, MA), and Bruker Compact QTOF (Bruker Daltonics, Billerica, MA) spectrometers with electron impact (EI), atmospheric pressure chemical ionization (APCI), and electrospray ionization (ESI), respectively. The single crystal X-ray diffraction measurements were performed on a Rigaku XtaLAB Synergy-R diffractometer (Rigaku, Tokyo, Japan) equipped with a HyPix-6000HE HPC detector with Mo Kα radiation (λ = 0.71073 Å) at 93 K.

Materials. All starting materials and anhydrous solvents were purchased from Sigma-Aldrich (St. Louis, MO), Fujifilm Wako Pure Chemical (Osaka, Japan), Tokyo Kasei (TCI, Tokyo, Japan), Nacalai Tesque (Kyoto, Japan), or Kanto Kagaku (Tokyo, Japan) and were used as received. (*R*,*R*)-, (*S*,*S*)-, and racemic (*rac*)-2,6-diiodotriptycene[S1] and *cis*-$(PEt_3)_2Pt(OTf)_2$ (**3**)[S2] were synthesized according to the previously reported methods.

2. Synthetic Procedures

(*R*,*R*)-, (*S*,*S*)-, and *rac*-**1** and -**2** were prepared according to Scheme S1.

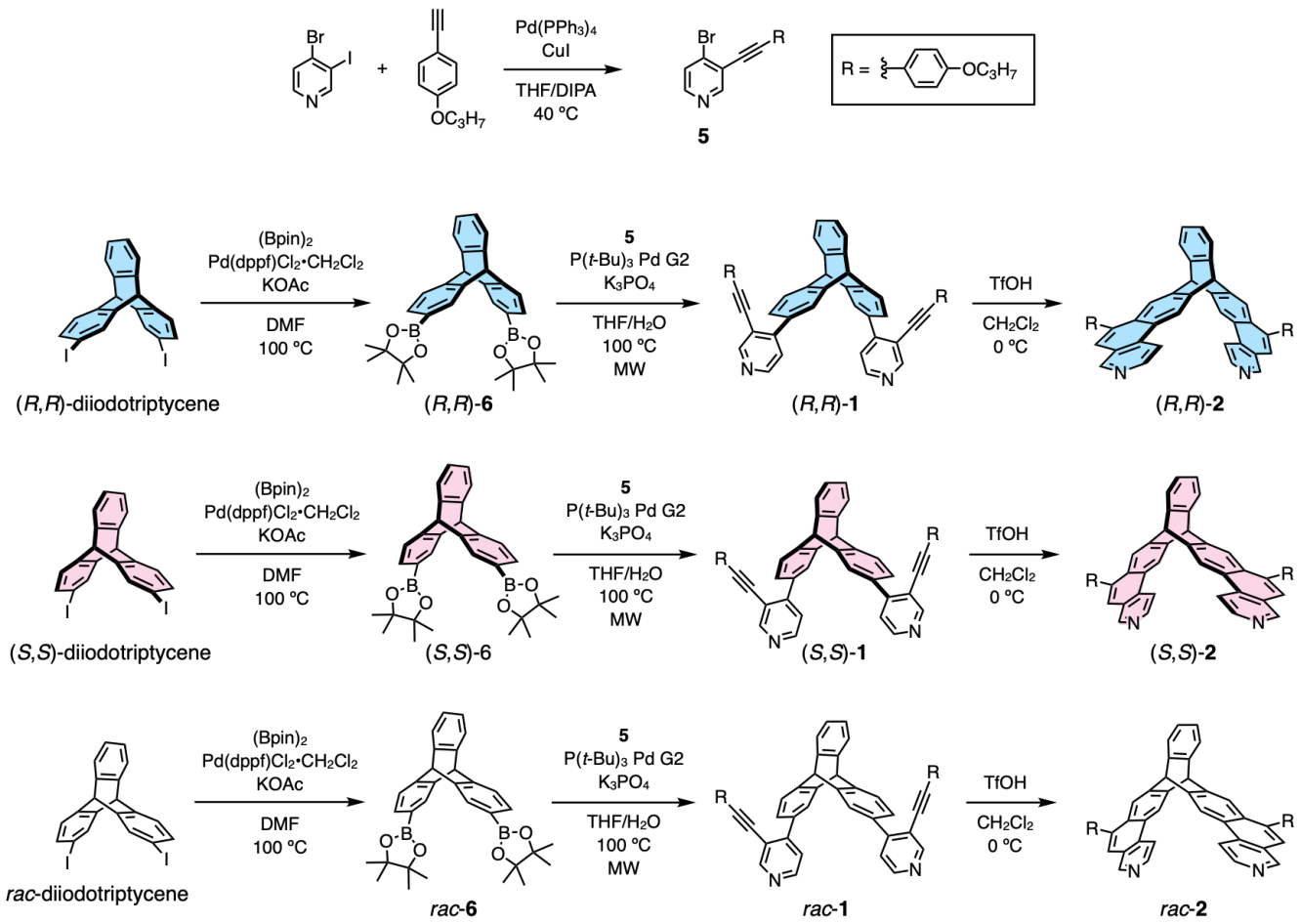

Scheme S1. Synthesis of (*R*,*R*)-, (*S*,*S*)-, and *rac*-**1** and -**2**.

Synthesis of 5. To a mixture of 4-bromo-3-iodopyridine (0.50 g, 1.8 mmol), copper (I) iodide (CuI) (7.0 mg, 37 μmol), and tetrakis(triphenylphosphine)palladium(0) ($Pd(PPh_3)_4$) (20 mg, 18 μmol) in a degassed tetrahydrofuran (THF)/diisopropylamine (DIPA) mixture (5/1, v/v; 6.0 mL) was added 1-ethynyl-4-propoxybenzene (0.30 g, 1.9 mmol). After stirring at 40 °C for 12 h, the mixture was diluted with chloroform and the solution was washed with water, and then dried over Na_2SO_4. The solvent was removed under reduced pressure and the crude product was purified by silica gel chromatography using *n*-hexane/ethyl acetate (1/1, v/v) as the eluent to give the desired product as a white solid (0.47 g, 84% yield). Mp: 46.4–47.0 °C. IR (KBr, cm^{-1}): 2219 (C≡C). ^{1}H NMR (500 MHz, $CDCl_3$, 25 °C): δ 8.68 (s, 1H, Ar–H), 8.29 (d, J = 5.4 Hz, 1H, Ar–H), 7.55 (d, J = 5.4 Hz, 1H, Ar–H), 7.53-7.50 (m, 2H, Ar–H), 6.91-6.88 (m, 2H, Ar–H), 3.96 (t, J = 6.6 Hz, 2H, CH_2), 1.83 (sext, J = 7.4 Hz, 2H, CH_2), 1.05 (t, J = 7.3 Hz, 3H, CH_3). ^{13}C NMR (126 MHz, $CDCl_3$, 25 °C): δ 159.95, 152.79, 148.17, 134.99, 133.30, 127.20,

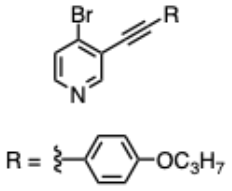

5

123.54, 114.65, 113.96, 97.47, 83.61, 69.61, 22.48, 10.45. HRMS (APCI+): *m*/*z* calcd for $C_{16}H_{14}BrNO$ ($M+H^+$), 316.0332; found 316.0338.

Synthesis of (*R*,*R*)-**6.** To a mixture of (*R*,*R*)-2,6-diiodotriptycene (0.10 g, 0.20 mmol), bis(pinacolato)diboron ($(Bpin)_2$) (0.13 g, 0.51 mmol), and potassium acetate (80 mg, 0.82 mmol) in anhydrous *N*,*N*-dimethylformamide (DMF) (2.0 mL) was added [1,1'-bis(diphenylphosphino)ferrocene]palladium(II) dichloride dichloromethane adduct ($Pd(dppf)Cl_2 \cdot CH_2Cl_2$) (6.0 mg, 7.3 μmol). After stirring at 100 °C for 12 h, the mixture was cooled to room temperature and diluted with dichloromethane. The solution was washed with water, and then dried over Na_2SO_4. The solvent was removed under reduced pressure and the crude product was purified by silica gel chromatography using *n*-hexane/chloroform (1/4, v/v) as the eluent to give the desired product as a white solid (0.081 g, 80% yield). Mp: >300 °C. $[\alpha]^{25}_D$ –39.1 (*c* 0.1, $CHCl_3$). ^{1}H NMR (500 MHz, $CDCl_3$, rt): δ 7.81 (s, 2H, Ar–H), 7.46 (dd, *J* = 7.2, 1.1 Hz, 2H, Ar–H), 7.36 (d, *J* = 7.1 Hz, 2H, Ar–H), 7.34-7.31 (m, 2H, Ar–H), 6.97-6.93 (m, 2H, Ar–H), 5.43 (s, 2H, CH), 1.29 (s, 24H, CH_3). ^{13}C NMR (126 MHz, $CDCl_3$, rt): δ 148.45, 144.74, 144.19, 132.36, 129.53, 125.18, 123.66, 123.13, 83.65, 54.17, 24.79. HRMS (EI+): *m*/*z* calcd for $C_{32}H_{36}B_2O_4$ (M^+), 506.2800; found 506.2790.

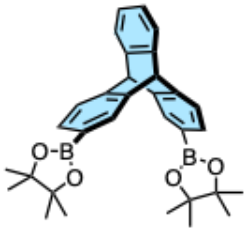
(*R*,*R*)-**6**

(*S*,*S*)- and *rac*-**6** were also prepared from (*S*,*S*)- and *rac*-2,6-diiodotriptycene with $(Bpin)_2$, respectively, in the same way for the synthesis of (*R*,*R*)-**6**.

Analytical data of (*S*,*S*)-**6**: White solid. Yield: 78%. Mp: >300 °C. $[\alpha]^{25}_D$ +40.6 (*c* 0.1, $CHCl_3$). ^{1}H NMR (500 MHz, $CDCl_3$, 25 °C): δ 7.81 (s, 2H, Ar–H), 7.46 (dd, *J* = 7.3, 1.2 Hz, 2H, Ar–H), 7.36 (d, *J* = 7.3 Hz, 2H, Ar–H), 7.35-7.31 (m, 2H, Ar–H), 6.97-6.94 (m, 2H, Ar–H), 5.43 (s, 2H, CH), 1.29 (s, 24H, CH_3). ^{13}C NMR (126 MHz, $CDCl_3$, rt): δ 148.45, 144.74, 144.19, 132.36, 129.53, 125.18, 123.66, 123.13, 83.64, 54.17, 24.79. HRMS (EI+): *m*/*z* calcd for $C_{32}H_{36}B_2O_4$ (M^+), 506.2800; found 506.2825.

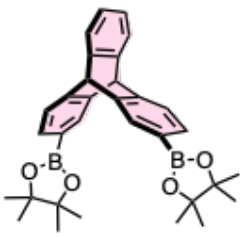
(*S*,*S*)-**6**

Analytical data of *rac*-**6**: White solid. Yield: 80%. Mp: >300 °C. ^{1}H NMR (500 MHz, $CDCl_3$, 25 °C): δ 7.81 (s, 2H, Ar–H), 7.46 (dd, *J* = 7.2, 1.1 Hz, 2H, Ar–H), 7.36 (d, *J* = 7.3 Hz, 2H, Ar–H), 7.34-7.31 (m, 2H, Ar–H), 6.97-6.93 (m, 2H, Ar–H), 5.43 (s, 2H, CH), 1.29 (s, 24H, CH_3). ^{13}C NMR (126 MHz, $CDCl_3$, rt): δ 148.45, 144.74, 144.19, 132.36, 129.53, 125.19, 123.66, 123.13, 83.64, 54.17, 24.79. HRMS (EI+): *m*/*z* calcd for $C_{32}H_{36}B_2O_4$ (M^+), 506.2800; found 506.2815.

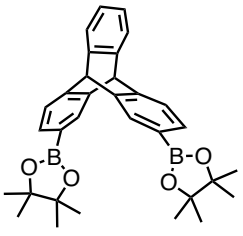
rac-**6**

Synthesis of (*R*,*R*)-**1**. To a mixture of (*R*,*R*)-**6** (51 mg, 0.10 mmol), **5** (66 mg, 0.21 mmol), and tripotassium phosphate (0.13 g, 0.60 mmol) in a degassed THF/H_2O mixture (4/1, v/v; 2.0 mL) was added chloro[(tri-*tert*-butylphosphine)-2-(2-aminobiphenyl)]palladium(II) (P(*t*-Bu)$_3$ Pd G2) (5.1 mg, 10 μmol). After stirring at 100 °C for 2 h in a microwave reactor, the mixture was diluted with dichloromethane and the solution was washed with brine, and then dried over Na_2SO_4. The solvent was removed under reduced pressure and the crude product was purified by silica gel chromatography using *n*-hexane/ethyl acetate (1/1, v/v) as the eluent to give the desired product as a pale yellow solid (55 mg, 76% yield). Mp: 165.6–166.2 °C. $[\alpha]^{25}_D$ –118.2º (*c* 0.1, $CHCl_3$). IR (KBr, cm^{-1}): 2216 (C≡C). ^{1}H NMR (500 MHz, $CDCl_3$, 25 °C): δ 8.78 (s, 2H, Ar–H), 8.50 (d, *J* = 5.1 Hz, 2H, Ar–H), 7.92 (d, *J* = 1.5 Hz, 2H, Ar–H), 7.52 (d, *J* = 7.6 Hz, 2H, Ar–H), 7.46-7.44 (m, 2H, Ar–H), 7.34 (dd, *J* = 7.6, 1.7 Hz, 2H, Ar–H), 7.28 (d, *J* = 5.1 Hz, 2H, Ar–H), 7.17-7.14 (m, 4H, Ar–H), 7.11-7.08 (m, 2H, Ar–H), 6.78-6.75 (m, 4H, Ar–H), 5.60 (s, 2H, CH), 3.89 (t, *J* = 6.6 Hz, 4H, CH_2), 1.80 (sext, *J* = 7.3 Hz, 4H, CH_2), 1.03 (t, *J* = 7.3 Hz, 6H, CH_3). ^{13}C NMR (126 MHz, $CDCl_3$, rt): δ 159.47, 153.22, 149.58, 148.20, 145.76, 144.92, 144.71, 135.16, 132.98, 125.93, 125.52, 124.46, 123.88, 123.70, 123.24, 118.73, 114.52, 114.45, 95.54, 84.91, 69.55, 53.96, 22.48, 10.47. HRMS (APCI+): *m*/*z* calcd for $C_{52}H_{40}N_2O_2$ (M+H$^+$), 725.3163; found 725.3180.

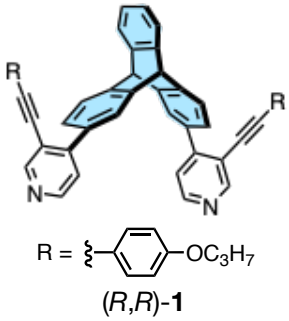

(*R*,*R*)-**1**

(*S*,*S*)- and *rac*-**1** were also prepared from (*S*,*S*)- and *rac*-**6** with **5**, respectively, in the same way for the synthesis of (*R*,*R*)-**1**.

Analytical data of (*S*,*S*)-**1**: Pale yellow solid. Yield: 72%. Mp: 164.8–165.5 °C. $[\alpha]^{25}_D$ +118.0 (*c* 0.1, $CHCl_3$). IR (KBr, cm^{-1}): 2216 (C≡C). ^{1}H NMR (500 MHz, $CDCl_3$, 25 °C): δ 8.78 (s, 2H, Ar–H), 8.49 (d, *J* = 5.1 Hz, 2H, Ar–H), 7.92 (d, *J* = 1.5 Hz, 2H, Ar–H), 7.52 (d, *J* = 7.8 Hz, 2H, Ar–H), 7.47-7.44 (m, 2H, Ar–H), 7.34 (dd, *J* = 7.6, 1.7 Hz, 2H, Ar–H), 7.27 (d, *J* = 5.4 Hz, 2H, Ar–H), 7.17-7.14 (m, 4H, Ar–H), 7.11-7.08 (m, 2H, Ar–H), 6.77-6.75 (m, 4H, Ar–H), 5.59 (s, 2H, CH), 3.89 (t, *J* = 6.6 Hz, 4H, CH_2), 1.80 (sext, *J* = 7.1 Hz, 4H, CH_2), 1.03 (t, *J* = 7.3 Hz, 6H, CH_3). ^{13}C NMR (126 MHz, $CDCl_3$, rt): δ 159.46, 153.24, 149.57, 148.22, 145.75, 144.91, 144.71, 135.16, 132.98, 125.93, 125.52, 124.46, 123.88, 123.70, 123.23, 118.71, 114.52, 114.45, 95.53, 84.91, 69.55, 53.96, 22.48, 10.47. HRMS (APCI+): *m*/*z* calcd for $C_{52}H_{40}N_2O_2$ (M+H$^+$), 725.3163; found 725.3187.

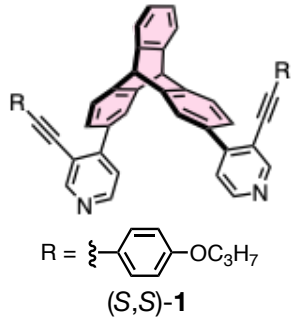

(*S*,*S*)-**1**

Analytical data of *rac*-**1**: Pale yellow solid. Yield: 70%. Mp: 165.5–166.2 °C. IR (KBr, cm^{-1}): 2216 (C≡C). ^{1}H NMR (500 MHz, $CDCl_3$, rt): δ 8.78 (s, 2H, Ar–H), 8.49 (d, J = 5.1 Hz, 2H, Ar–H), 7.92 (d, J = 1.7 Hz, 2H, Ar–H), 7.52 (d, J = 7.6 Hz, 2H, Ar–H), 7.47-7.44 (m, 2H, Ar–H), 7.34 (dd, J = 7.6, 1.7 Hz, 2H, Ar–H), 7.28 (d, J = 5.1 Hz, 2H, Ar–H), 7.17-7.14 (m, 4H, Ar–H), 7.11-7.08 (m, 2H, Ar–H), 6.78-6.75 (m, 4H, Ar–H), 5.59 (s, 2H, CH), 3.89 (t, J = 6.6 Hz, 4H, CH_2), 1.80 (sext, J = 7.0 Hz, 4H, CH_2), 1.03 (t, J = 7.4 Hz, 6H, CH_3). ^{13}C NMR (126 MHz, $CDCl_3$, rt): δ 159.46, 153.11, 149.46, 147.97, 145.75, 144.90, 144.69, 135.18, 132.98, 125.90, 125.51, 124.43, 123.87, 123.70, 123.23, 118.72, 114.52, 114.42, 95.61, 84.98, 69.54, 53.95, 22.48, 10.46. HRMS (APCI+): *m*/*z* calcd for $C_{52}H_{40}N_2O_2$ ($M+H^+$), 725.3163; found 725.3178.

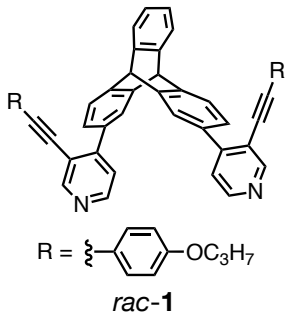

rac-**1**

Synthesis of (*R*,*R*)-**2.** (*R*,*R*)-**1** (40 mg, 55 μmol) was dissolved in an anhydrous dichloromethane/trifluoromethanesulfonic acid (TfOH) mixture (40/1, v/v; 10.0 mL) and the solution was stirred at 0 ºC for 1 h. After quenching the reaction with saturated aqueous $NaHCO_3$, the mixture was diluted with dichloromethane and the solution was washed with saturated aqueous $NaHCO_3$ and water, and then dried over Na_2SO_4. The solvent was removed under reduced pressure and the product was passed through a short pad of silica gel using *n*-hexane/ethyl acetate (1/2, v/v) as the eluent to give the desired product as a pale yellow solid (37 mg, 92% yield). Mp: >300 °C. $[\alpha]^{25}_D$ –112.7 (*c* 0.1, $CHCl_3$). ^{1}H NMR (500 MHz, $CDCl_3$, 25 °C): δ 9.17 (s, 2H, Ar–H), 8.74 (s, 2H, Ar–H), 8.70 (d, J = 5.9 Hz, 2H, Ar–H), 8.37 (d, J = 6.1 Hz, 2H, Ar–H), 8.04 (s, 2H, Ar–H), 7.65 (s, 2H, Ar–H), 7.51-7.48 (m, 2H, Ar–H), 7.41-7.38 (m, 4H, Ar–H), 7.12-7.09 (m, 4H, Ar–H), 7.08-7.05 (m, 2H, Ar–H), 5.80 (s, 2H, CH), 4.08 (t, J = 6.5 Hz, 4H, CH_2), 1.93 (sext, J = 7.1 Hz, 4H, CH_2), 1.15 (t, J = 7.4 Hz, 6H, CH_3). ^{13}C NMR (126 MHz, $CDCl_3$, rt): δ 158.91, 151.86, 144.64, 144.55, 143.74, 142.85, 140.06, 133.93, 132.27, 131.50, 131.02, 126.90, 126.03, 125.08, 124.14, 121.75, 118.30, 115.72, 114.49, 69.71, 53.91, 22.71, 10.65. HRMS (APCI+): *m*/*z* calcd for $C_{52}H_{40}N_2O_2$ ($M+H^+$), 725.3163; found 725.3188.

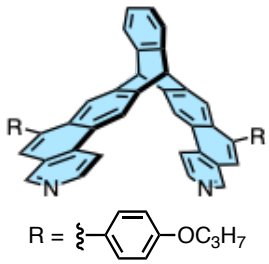

(*R*,*R*)-**2**

(*S*,*S*)- and *rac*-**2** were also prepared from (*S*,*S*)- and *rac*-**1**, respectively, in the same way for the synthesis of (*R*,*R*)-**2**.

Analytical data of (*S*,*S*)-**2**: Pale yellow solid. Yield: 94%. Mp: >300 °C. $[\alpha]^{25}_{D}$ +111.1 (*c* 0.1, $CHCl_3$). ^1H NMR (500 MHz, $CDCl_3$, 25 °C): δ 9.17 (s, 2H, Ar–H), 8.74 (s, 2H, Ar–H), 8.69 (d, *J* = 5.9 Hz, 2H, Ar–H), 8.37 (d, *J* = 5.9 Hz, 2H, Ar–H), 8.04 (s, 2H, Ar–H), 7.65 (s, 2H, Ar–H), 7.50-7.48 (m, 2H, Ar–H), 7.41-7.38 (m, 4H, Ar–H), 7.12-7.09 (m, 4H, Ar–H), 7.08-7.05 (m, 2H, Ar–H), 5.80 (s, 2H, CH), 4.08 (t, *J* = 6.5 Hz, 4H, CH_2), 1.93 (sext, *J* = 7.1 Hz, 4H, CH_2), 1.15 (t, *J* = 7.4 Hz, 6H, CH_3). ^{13}C NMR (126 MHz, $CDCl_3$, rt): δ 158.92, 151.86, 144.65, 144.56, 143.74, 142.86, 140.06, 133.94, 132.28, 131.51, 131.03, 126.91, 126.04, 125.09, 124.15, 121.76, 118.31, 115.73, 114.50, 69.71, 53.92, 22.72, 10.66. HRMS (APCI+): *m*/*z* calcd for $C_{52}H_{40}N_2O_2$ ($M+H^+$), 725.3163; found 725.3178.

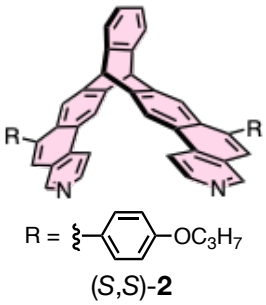

(*S*,*S*)-**2**

Analytical data of *rac*-**2**: Pale yellow solid. Yield: 90%. Mp: >300 °C. ^1H NMR (500 MHz, $CDCl_3$, 25 °C): δ 9.17 (s, 2H, Ar–H), 8.74 (s, 2H, Ar–H), 8.70 (d, *J* = 5.9 Hz, 2H, Ar–H), 8.38 (d, *J* = 6.1 Hz, 2H, Ar–H), 8.04 (s, 2H, Ar–H), 7.65 (s, 2H, Ar–H), 7.51-7.49 (m, 2H, Ar–H), 7.41-7.39 (m, 4H, Ar–H), 7.11-7.09 (m, 4H, Ar–H), 7.08-7.05 (m, 2H, Ar–H), 5.80 (s, 2H, CH), 4.08 (t, *J* = 6.6 Hz, 4H, CH_2), 1.93 (sext, *J* = 6.9 Hz, 4H, CH_2), 1.15 (t, *J* = 7.3 Hz, 6H, CH_3). ^{13}C NMR (126 MHz, $CDCl_3$, rt): δ 158.91, 151.84, 144.63, 144.53, 143.73, 142.84, 140.05, 133.92, 132.25, 131.50, 131.01, 126.90, 126.02, 125.08, 124.14, 121.75, 118.30, 115.74, 114.49, 69.70, 53.90, 22.70, 10.65. HRMS (APCI+): *m*/*z* calcd for $C_{52}H_{40}N_2O_2$ ($M+H^+$), 725.3163; found 725.3169.

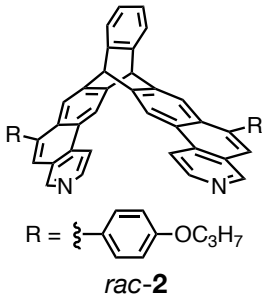

rac-**2**

(*R*,*R*,*R*,*R*)-, (*S*,*S*,*S*,*S*)-, and *rac*-**4** were prepared according to Scheme S2.

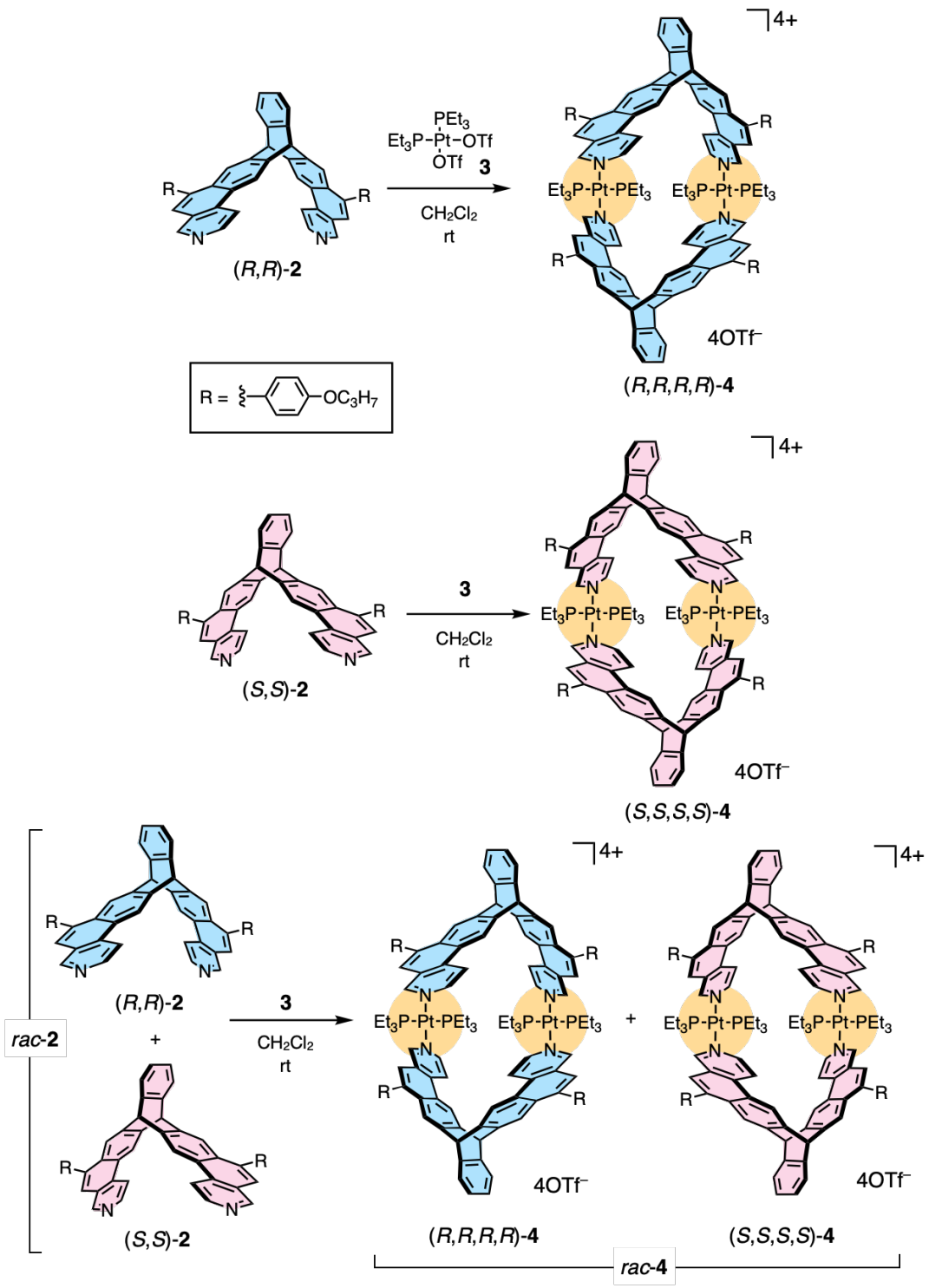

Scheme S2. Synthesis of (*R*,*R*,*R*,*R*)-, (*S*,*S*,*S*,*S*)-, and *rac*-**4**.

Synthesis of (*R*,*R*,*R*,*R*)-**4.** (*R*,*R*)-**2** (3.2 mg, 4.4 μmol) and **3** (3.2 mg, 4.4 μmol) were dissolved in dichloromethane (1.0 mL) and the solution was stirred at room temperature for 3 h. After removing the solvent by evaporation, the desired product was quantitatively obtained as a pale yellow solid (6.4 mg, >99% yield). Mp: decomposed at > 260 °C. $[\alpha]^{25}_{D}$ –282.1 (*c* 0.05, $CHCl_3$). ^{1}H NMR (500 MHz, $CDCl_3$, 25 °C): δ 9.98 (d, J = 2.3 Hz, 4H, Ar–H), 9.37 (d, J = 5.1 Hz, 4H, Ar–H), 8.46 (s, 4H, Ar–H), 8.41 (d, J = 6.8 Hz, 4H, Ar–H), 7.99 (s, 4H, Ar–H), 7.93 (s, 4H, Ar–H), 7.43-7.39 (m, 4H, Ar–H), 7.31-7.29 (m, 8H, Ar–H), 7.13-7.11 (m, 8H, Ar–H), 7.05-7.02 (m, 4H, Ar–H), 5.61 (s, 4H, CH), 4.10 (t, J = 6.6 Hz, 8H, CH_2), 1.99-1.85 (m, 32H, CH_2), 1.35-1.26 (m, 36H, CH_2), 1.17 (t, J = 7.4 Hz, 12H, CH_3). ^{13}C NMR (126 MHz, $CDCl_3$, rt): δ 159.44, 152.88, 146.28, 143.21, 143.11, 142.89, 142.58, 134.83, 132.57, 130.99, 130.45, 128.51, 126.24, 125.30, 124.40, 124.32, 122.30, 121.96, 120.15, 119.76, 119.02, 114.87, 69.76, 53.54, 22.77, 15.79, 15.63, 15.49, 10.67, 7.72. HRMS (ESI+): *m*/*z* calcd for $C_{128}H_{140}N_4O_4P_4Pt_2$ ($[M–4OTf^-]^{4+}$), 577.7275; found 577.7274.

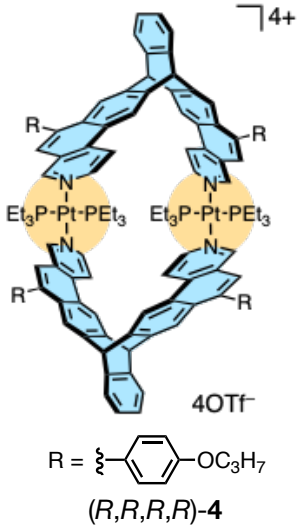

(*R*,*R*,*R*,*R*)-**4**

(*S*,*S*,*S*,*S*)- and *rac*-**4** were also prepared from (*S*,*S*)- and *rac*-**2** with **3**, respectively, in the same way for the synthesis of (*R*,*R*,*R*,*R*)-**4**.

Analytical data of (*S*,*S*,*S*,*S*)-**4**: Pale yellow solid. Yield: 99%. Mp: decomposed at > 260 °C. $[\alpha]^{25}_{D}$ +282.0 (*c* 0.05, $CHCl_3$). ^{1}H NMR (500 MHz, $CDCl_3$, 25 °C): δ 9.98 (d, J = 2.4 Hz, 4H, Ar–H), 9.37 (d, J = 5.4 Hz, 4H, Ar–H), 8.46 (s, 4H, Ar–H), 8.41 (d, J = 6.6 Hz, 4H, Ar–H), 7.99 (s, 4H, Ar–H), 7.93 (s, 4H, Ar–H), 7.42-7.40 (m, 4H, Ar–H), 7.31-7.29 (m, 8H, Ar–H), 7.13-7.11 (m, 8H, Ar–H), 7.05-7.03 (m, 4H, Ar–H), 5.61 (s, 4H, CH), 4.10 (t, J = 6.6 Hz, 8H, CH_2), 1.99-1.85 (m, 32H, CH_2), 1.35-1.29 (m, 36H, CH_2), 1.17 (t, J = 7.4 Hz, 12H, CH_3). ^{13}C NMR (126 MHz, $CDCl_3$, rt): δ 159.44, 152.88, 146.28, 143.20, 143.12, 142.90, 142.58, 134.83, 132.57, 130.99, 130.46, 128.52, 126.25, 125.31, 124.40, 124.33, 122.31, 121.97, 120.16, 119.77, 119.02, 114.88, 69.76, 53.55, 22.78, 15.80, 15.64, 15.50, 10.68, 7.73. HRMS (ESI+): *m*/*z* calcd for $C_{128}H_{140}N_4O_4P_4Pt_2$ ($[M–4OTf^-]^{4+}$), 577.7275; found 577.7265.

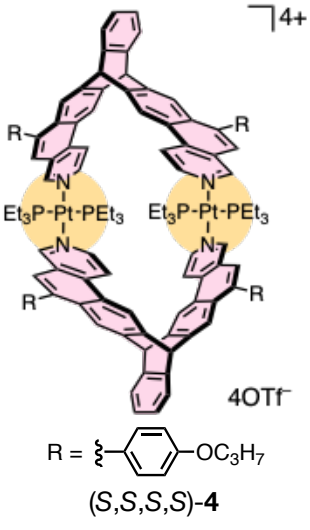

(*S*,*S*,*S*,*S*)-**4**

Analytical data of *rac*-**4**: Pale yellow solid. Yield: 98%. Mp: decomposed at > 260 °C. ^{1}H NMR

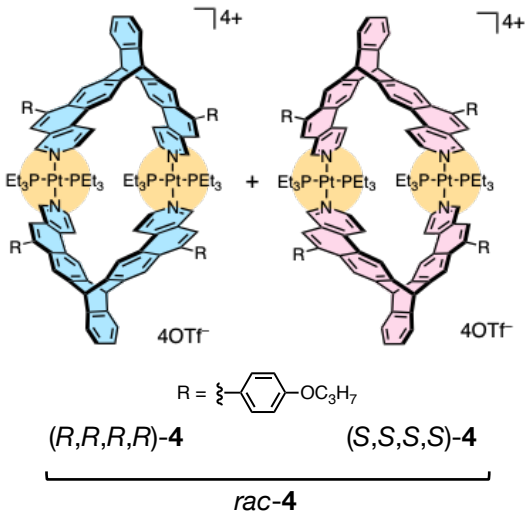

(500 MHz, $CDCl_3$, 25 °C): δ 9.98 (d, J = 2.4 Hz, 4H, Ar–H), 9.37 (d, J = 4.9 Hz, 4H, Ar–H), 8.46 (s, 4H, Ar–H), 8.40 (d, J = 6.7 Hz, 4H, Ar–H), 7.99 (s, 4H, Ar–H), 7.93 (s, 4H, Ar–H), 7.42-7.40 (m, 4H, Ar–H), 7.31-7.29 (m, 8H, Ar–H), 7.13-7.11 (m, 8H, Ar–H), 7.05-7.02 (m, 4H, Ar–H), 5.61 (s, 4H, CH), 4.10 (t, J = 6.4 Hz, 8H, CH_2), 1.99-1.81 (m, 32H, CH_2), 1.35-1.27 (m, 36H, CH_2), 1.17 (t, J = 7.5 Hz, 12H, CH_3). ^{13}C NMR (126 MHz, $CDCl_3$, rt): δ 159.44, 152.89, 146.28, 143.21, 143.11, 142.90, 142.58, 134.83, 132.57, 130.99, 130.45, 128.53, 126.25, 125.31, 124.40, 124.33, 122.30, 121.97, 120.15, 119.76, 119.02, 114.88, 69.77, 53.55, 22.78, 15.81, 15.64, 15.51, 10.68, 7.73. HRMS (ESI+): *m*/*z* calcd for $C_{128}H_{140}N_4O_4P_4Pt_2$ ($[M–4OTf^–]^{4+}$), 577.7275; found 577.7255.

3. X-ray Crystallographic Data of *rac*-4

X-ray diffraction data set for *rac*-**4** was collected on a Rigaku XtaLAB Synergy-R diffractometer with Mo Kα radiation (λ = 0.71073 Å) at 93 K. Single crystals of *rac*-**4** suitable for X-ray analysis were grown by vapor diffusion of *n*-hexane into a solution of *rac*-**4** in dichloromethane, and a single colorless crystal with dimensions 0.16 × 0.05 × 0.04 mm^3 was selected for intensity measurements. The unit cell was triclinic with the space group *P*2/*c*. Lattice constants with Z = 2, ρ_{calcd} = 1.367 g cm^{-3}, μ(Mo$_{K\alpha}$) = 2.157 mm^{-1}, F(000) = 2,952, 2θ_{max} = 50.998° were a = 17.7093(5) Å, b = 16.7013(6), c = 23.8942(6) Å, α = 90°, β = 91.581(2)°, γ = 90° and V = 7064.5(4) Å^3. A total of 52,497 reflections was collected, of which 13,158 reflections were independent (R_{int} = 0.0824). The structure was refined to final R_1 = 0.0891 for 7,129 data [I>2σ(I)] with 1,053 parameters and wR_2 = 0.2807 for all data, *GOF* = 1.043, and residual electron density max/min = 1.909/–1.018 e Å^{-3}. The perspective view is shown in Fig. 3 and crystal data and structure refinement are listed in Table S1.

Data collection and processing were conducted using the Rigaku CrysAlisPro software package.[S3] The structure was solved by direct methods using SHLEXT-2018/2[S4,S5] and refined by full-matrix least squares methods with SHELXL-2018/3 program[S6,S7] using Olex2-1.3.[S8] All non-hydrogen atoms were refined anisotropically. All hydrogen atoms were calculated geometrically and refined using the riding model. Crystallographic data have been deposited at the CCDC (12 Union Road, Cambridge CB2 1EZ, UK) and copies can be obtained on request, free of charge, by quoting the publication citation and the deposition number 2258185.

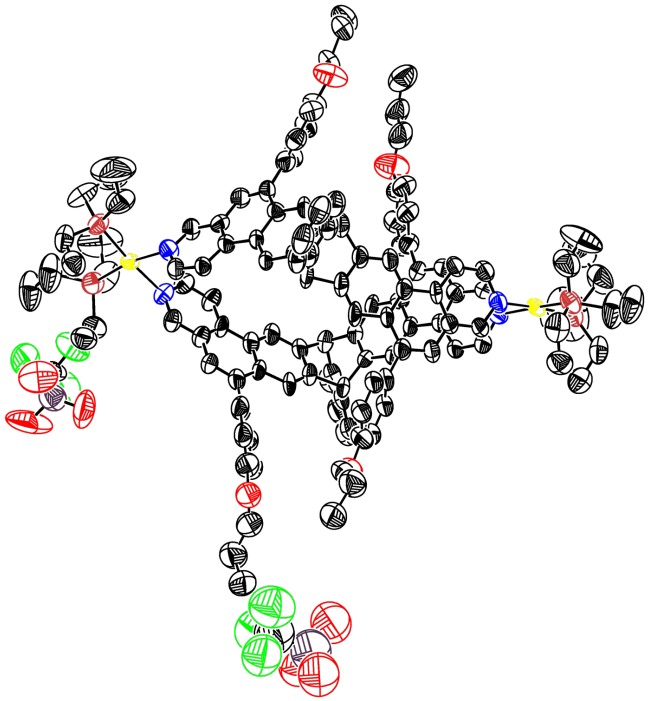

ORTEP drawing of the crystal structure of *rac*-**4** with thermal ellipsoids at 50% probability

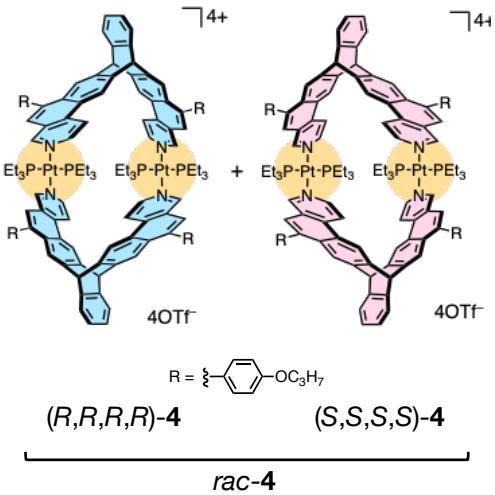

Table S1: Crystal data and structure refinement for *rac*-**4**.

Empirical formula	$C_{132}H_{140}F_{12}N_4O_{16}P_4Pt_2S_4$	
Formula weight	2908.77	
Temperature	93 K	
Wavelength	0.71073 Å	
Crystal system	monoclinic	
Space group	*P*2/*c*	
Unit cell dimensions	a = 17.7093(5) Å	α = 90°
	b = 16.7013(6) Å	β = 91.581(2)°
	c = 23.8942(6) Å	γ = 90°
Volume	7064.5(4) Å^3	
Z	2	
Density (calculated)	1.367 g cm^{-3}	
Absorption coefficient	2.157 mm^{-1}	
F(000)	2,952	
Crystal size	0.16 × 0.05 × 0.04 mm^3	
Theta range for data collection	1.676 to 25.499°	
Reflections collected	52,497	
Independent reflections	13,158 [R_{int} = 0.0824]	
Parameters	1,053	
Goodness-of-fit on F^2	1.043	
Final R indices [I>2sigma(I)]	R_1 = 0.0891, wR_2 = 0.2502	
R indices (all data)	R_1 = 0.1520, wR_2 = 0.2807	
Largest diff. peak and hole	1.909 and –1.018 eÅ^{-3}	
CCDC reference number	2258185	

4. Supporting Data

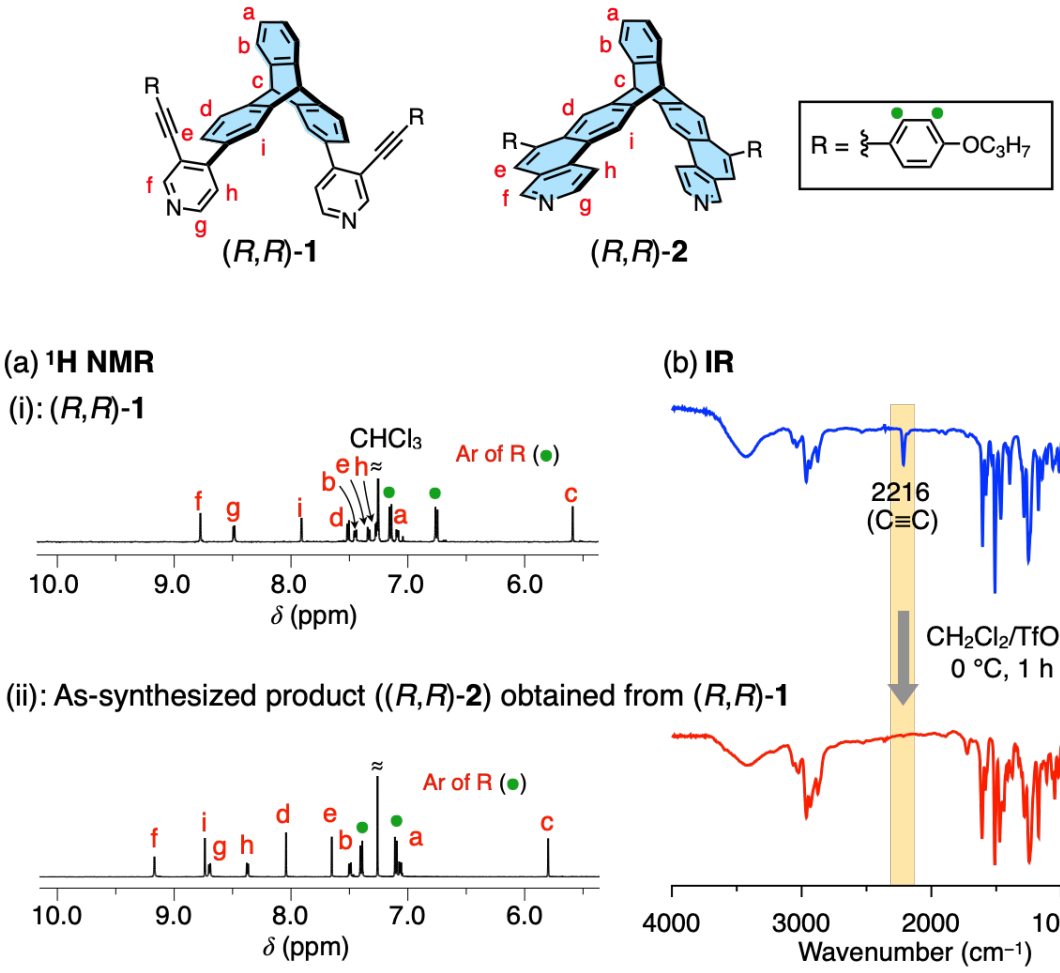

Fig. S1. (a) ^{1}H NMR (500 MHz, $CDCl_3$, 25 °C) and (b) IR (KBr, rt) spectra of (*R*,*R*)-**1** (i) and those of the as-synthesized product ((*R*,*R*)-**2**) (ii) after acid-promoted cyclizations in a dichloromethane/TfOH (40/1, v/v) mixture at 0 ºC for 1 h. For the signal assignments of (a), see Fig. S2a,b.

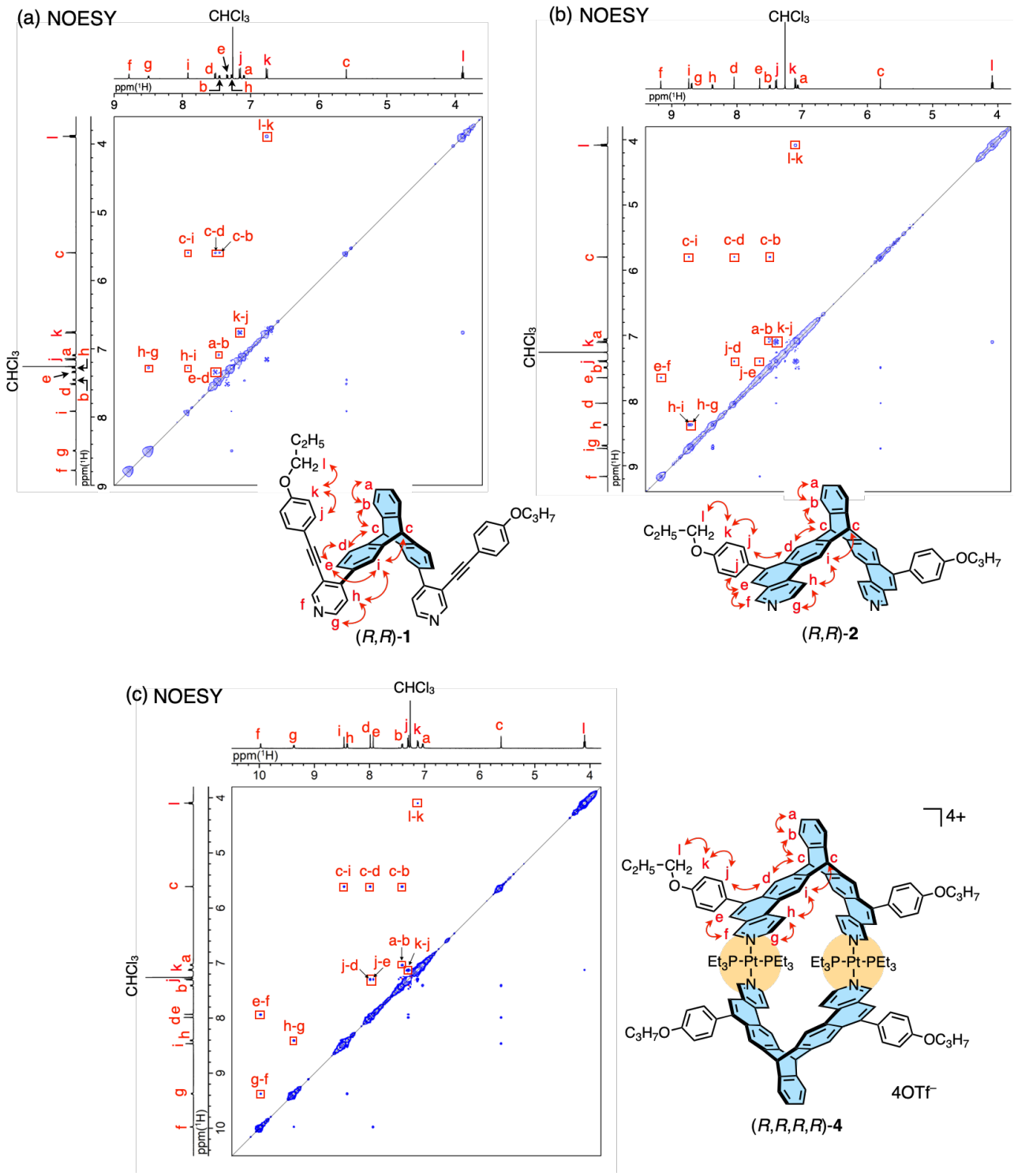

Fig. S2. Partial NOESY spectra (500 MHz, $CDCl_3$, rt, mixing time = 500 ms) of (*R*,*R*)-**1** (a), (*R*,*R*)-**2** (b), and (*R*,*R*,*R*,*R*)-**4** (c).

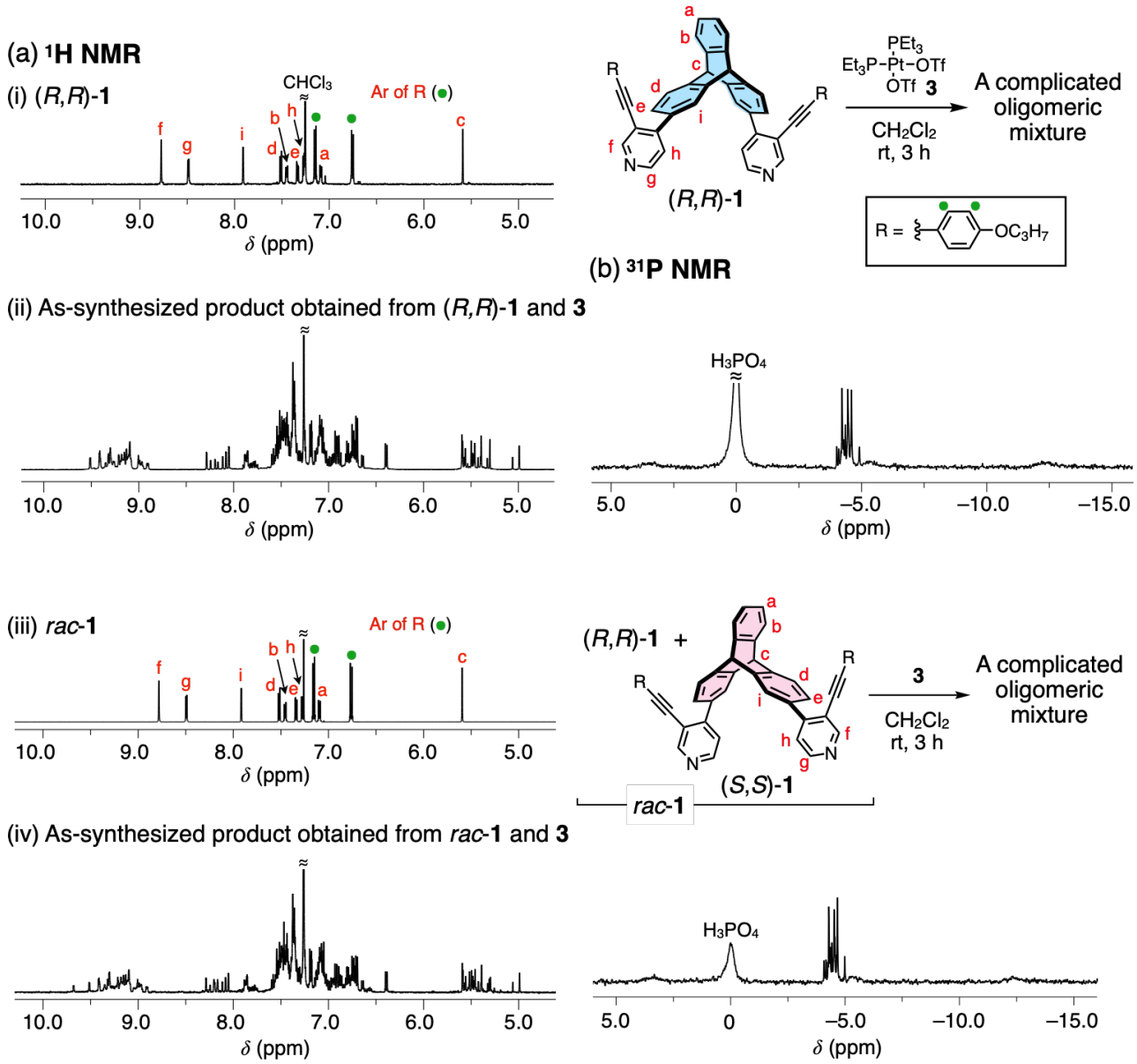

Fig. S3. ^{1}H (a; 500 MHz, $CDCl_3$, 25 °C) and/or ^{31}P (b; 203 MHz, $CDCl_3$, rt) NMR spectra of (*R*,*R*)-**1** (i), *rac*-**1** (iii), and the as-synthesized products (ii,iv) after complexation reaction with **3** in dichloromethane at room temperature for 3 h.

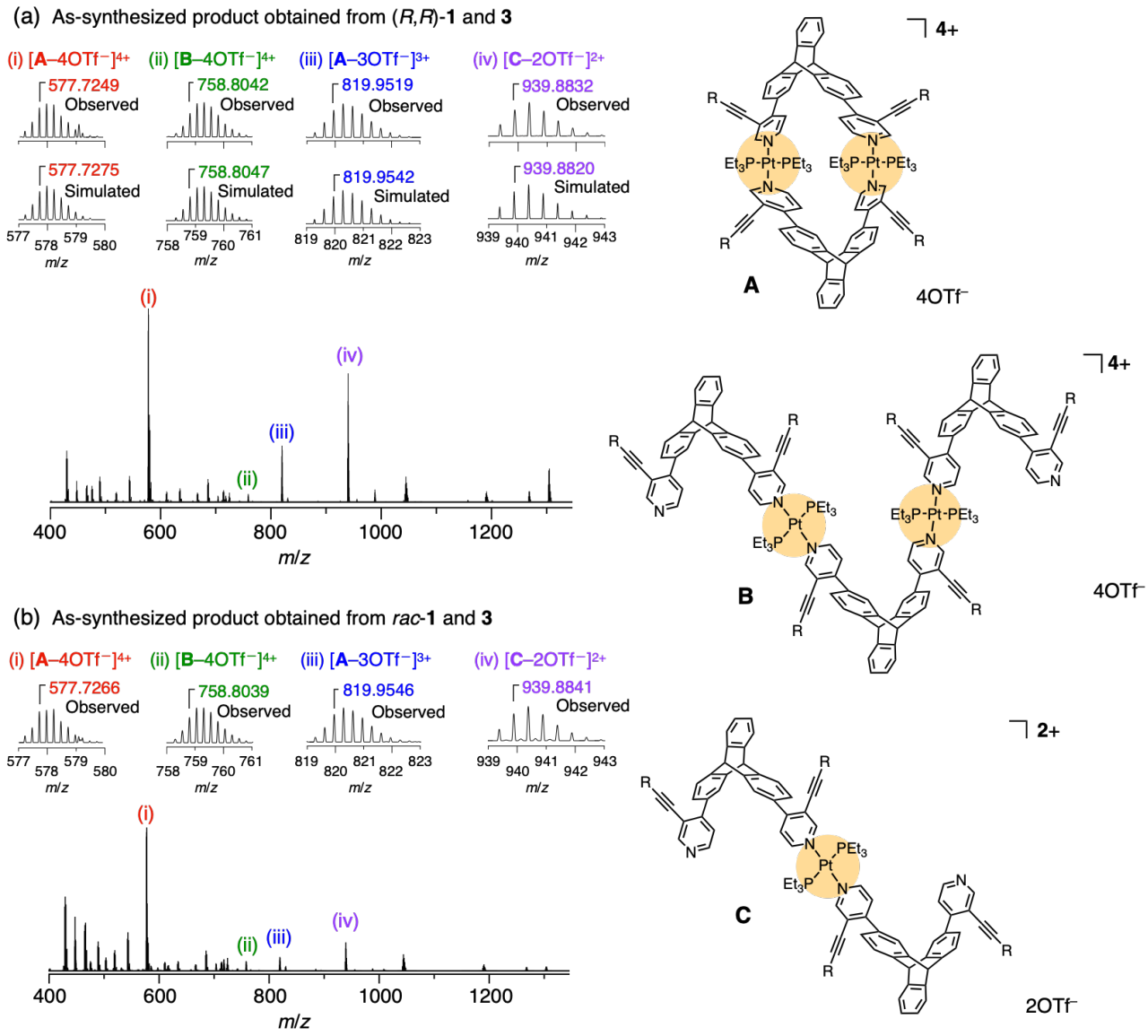

Fig. S4. Positive mode ESI-MS spectra of the as-synthesized products obtained through coordination-driven self-assembly of (*R*,*R*)-**1** (a) and *rac*-**1** (b) with an equivalent amount of **3**.

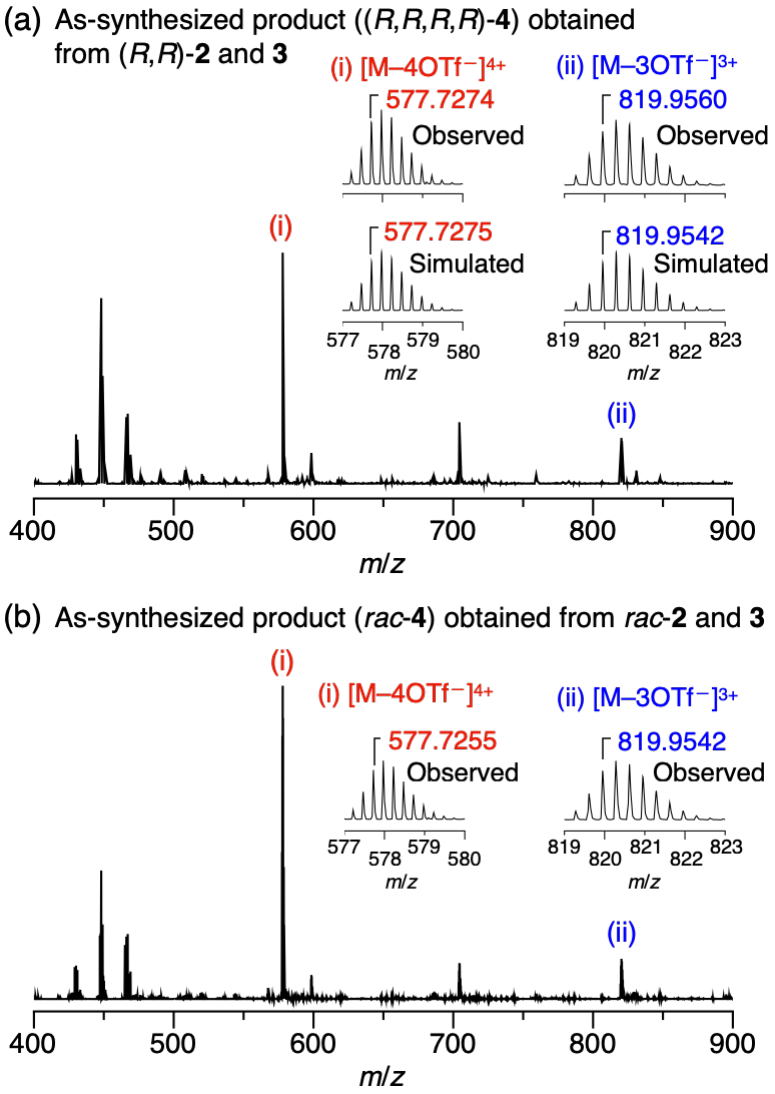

Fig. S5. Positive mode ESI-MS spectra of the as-synthesized products ((*R*,*R*,*R*,*R*)-**4** (a) and *rac*-**4** (b)) obtained through coordination-driven self-assembly of (*R*,*R*)-**2** and *rac*-**2** with an equivalent amount of **3**, respectively.

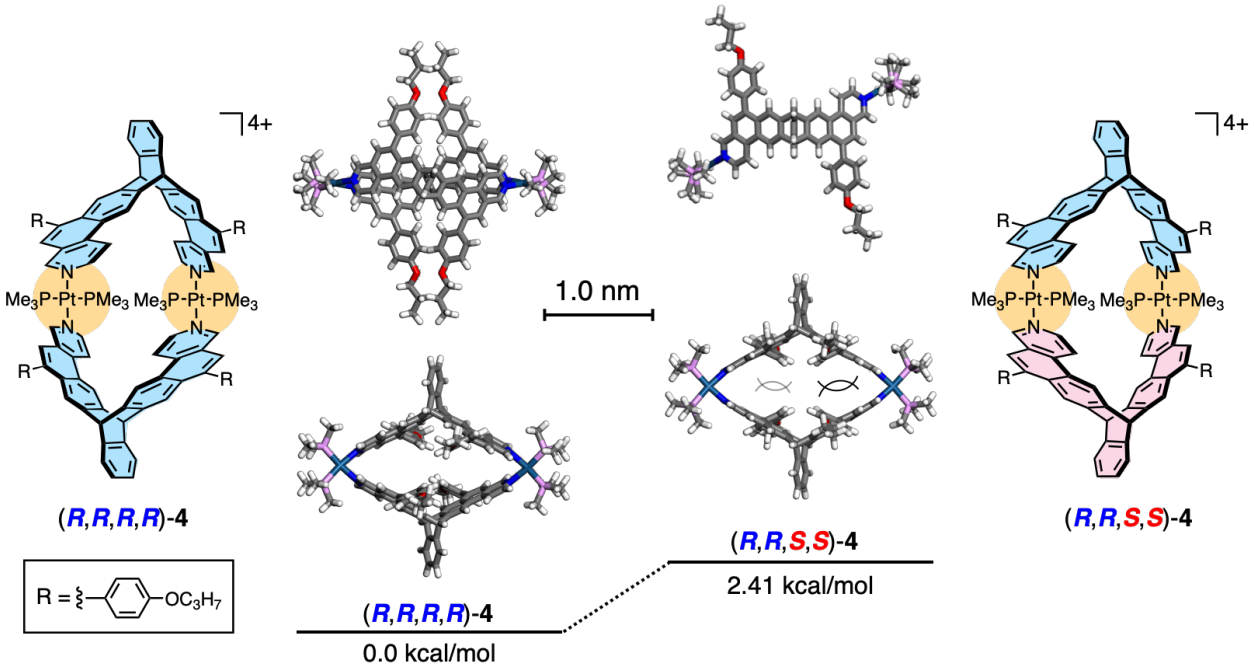

Fig. S6. Energy-minimized structures of (*R*,*R*,*R*,*R*)- and (*R*,*R*,*S*,*S*)-**4** obtained by DFT calculations at the B3LYP/6-31G(d,p) (for C, H, N, O, P) and B3LYP/LanL2DZ (for Pt) levels, in which the ethyl groups of the phosphine ligands were replaced by the methyl groups for simplicity. The triflate counter anions are not included in the calculations. The energy difference values are also shown.

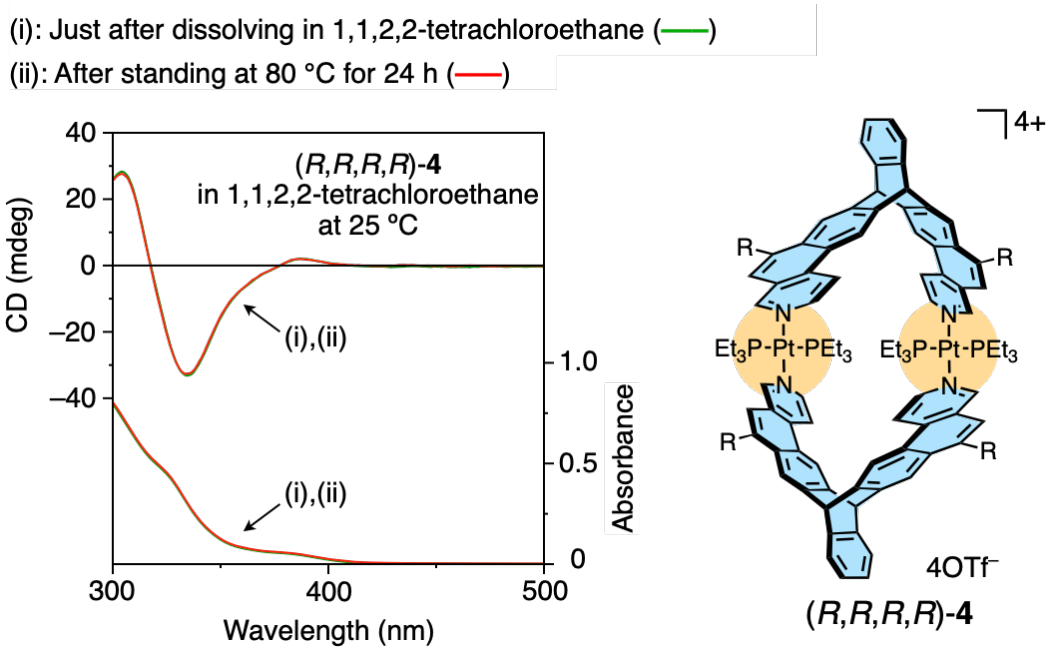

Fig. S7. CD and absorption spectra of (*R*,*R*,*R*,*R*)-**4** in 1,1,2,2-tetrachloroethane measured at 25 °C before (i) and after (ii) allowing to stand at 80 °C for 24 h. [(*R*,*R*,*R*,*R*)-**4**] = ca. 8×10^{-5} M.

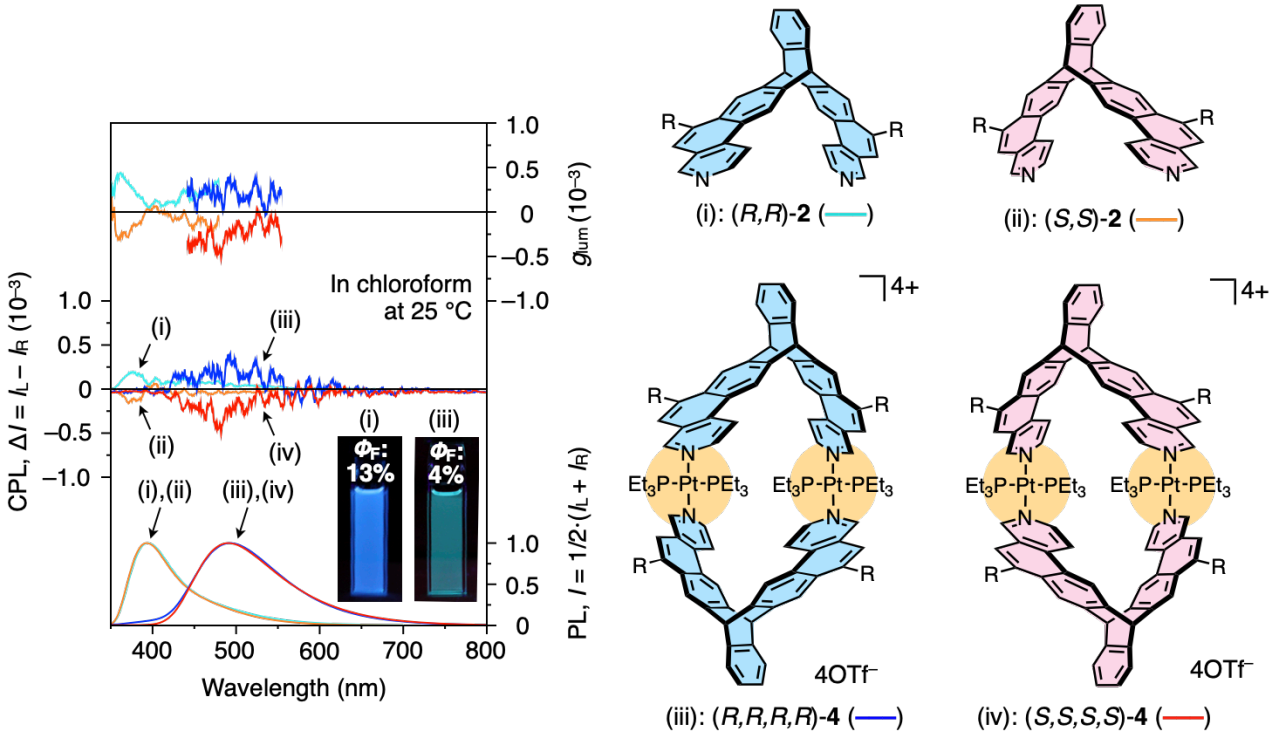

Fig. S8. Normalized PL (bottom), CPL (middle), and g_{lum} (top) spectra of (*R*,*R*)-**2** (i), (*S*,*S*)-**2** (ii), (*R*,*R*,*R*,*R*)-**4** (iii), and (*S*,*S*,*S*,*S*)-**4** (iv) in chloroform at 25 °C. The g_{lum} values are defined as $2(I_L - I_R)/(I_L + I_R)$, where I_L and I_R are the PL intensities of the left- and right-handed circularly polarized light, respectively. λ_{ex} = 300 nm. The insets show photographs of (*R*,*R*)-**2** and (*R*,*R*,*R*,*R*)-**4** in chloroform under irradiation at 365 nm. Fluorescence quantum yields (Φ_F) are also shown. [(*R*,*R*)-**2**] = 1.0×10^{-5} M; [(*R*,*R*,*R*,*R*)-**4**] = 0.50×10^{-5} M.

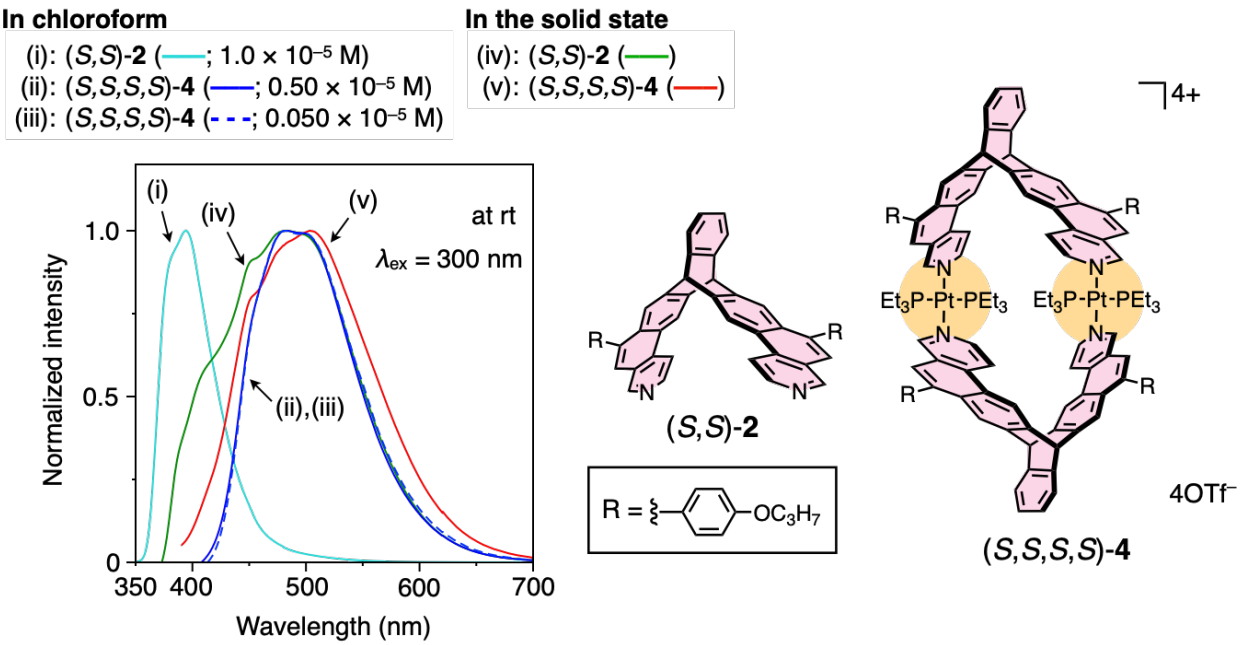

Fig. S9. Normalized PL spectra of (*S*,*S*)-**2** (i, iv) and (*S*,*S*,*S*,*S*)-**4** (ii, iii, v) in chloroform (i–iii) and in the solid state (iv, v) at room temperature. λ_{ex} = 300 nm.

The PL band centered at 500 nm of (*S*,*S*,*S*,*S*)-**4** remained almost unchanged over the concentration range of 0.050–0.50 × 10^{-5} M in chloroform and even in the solid state (Fig. S9(ii,iii,v)). On the other hand, the PL spectrum of the corresponding ligand ((*S*,*S*)-**2**) in the solid state was remarkably red-shifted compared to that in chloroform (Fig. S9(i,iv)) as observed in the PL spectrum of (*S*,*S*,*S*,*S*)-**4** in chloroform (Fig. S9(ii, iii)). These results indicate that the 500-nm PL band of (*S*,*S*,*S*,*S*)-**4** is most likely derived from an excimer emission of the two triptycene ligands in the metallomacrocycle arranging in close proximity to each other.

5. Supporting References

S1. T. Ikai, T. Yoshida, K. Shinohara, T. Taniguchi, Y. Wada and T. M. Swager, *J. Am. Chem. Soc.*, 2019, **141**, 4696–4703.

S2. P. J. Stang, D. H. Cao, S. Saito and A. M. Arif, *J. Am. Chem. Soc.*, 1995, **117**, 6273–6283.

S3. CrysAlisPRO, Oxford Diffraction/Agilent Technologies UK Ltd, Yarnton, England, 2015.

S4. G. Sheldrick, *Acta Crystallogr. Sect. A*, 2008, **64**, 112–122.

S5. G. Sheldrick, *Acta Crystallogr. Sect. A*, 2015, **71**, 3–8.

S6. G. Sheldrick, *Acta Crystallogr. Sect. C-Struct. Chem.*, 2015, **71**, 3–8.

S7. G. Sheldrick, SHELXL-2018/3: Program for the Refinement of Crystal Structures; University of Göttingen, Göttingen, Germany, 2018.

S8. O. V. Dolomanov, L. J. Bourhis, R. J. Gildea, J. A. K. Howard and H. Puschmann, *J. Appl. Cryst.*, 2009, **42**, 339–341.

6. ^{1}H and ^{13}C NMR Spectral Data

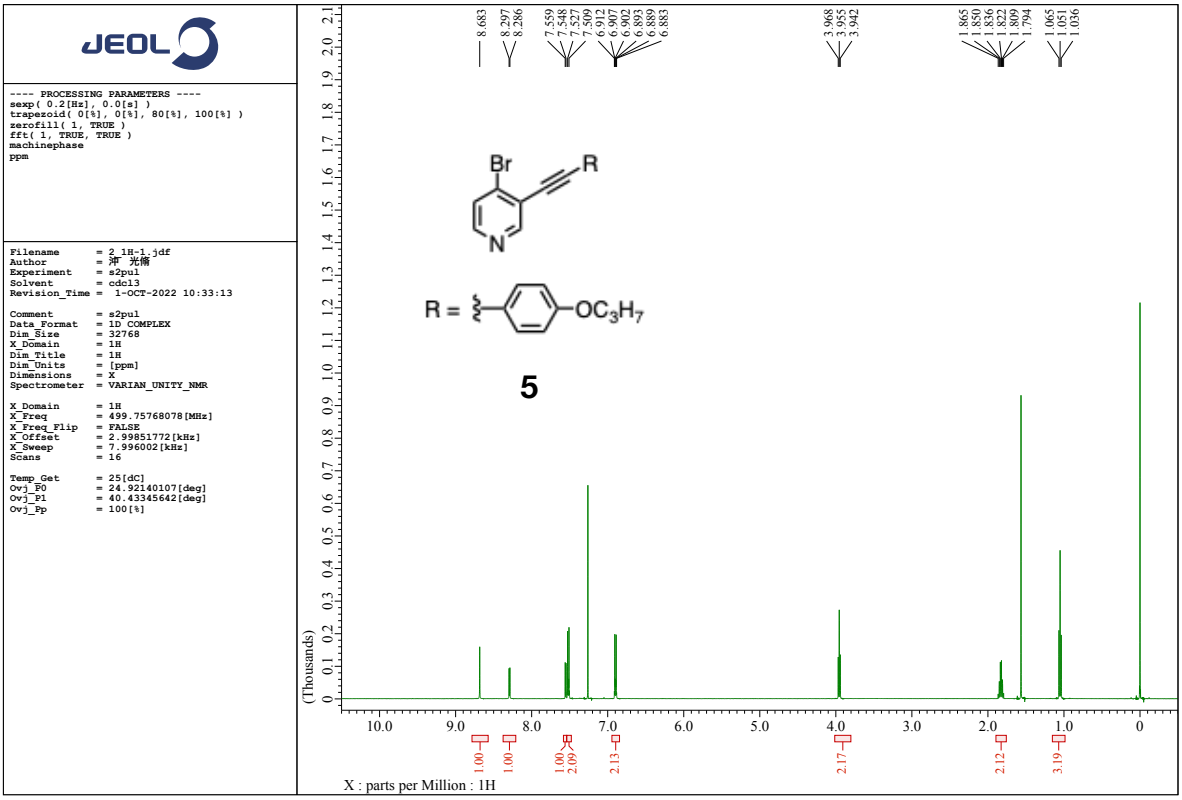

Fig. S10. ^{1}H NMR (500 MHz, $CDCl_3$, 25 °C) spectrum of **5**.

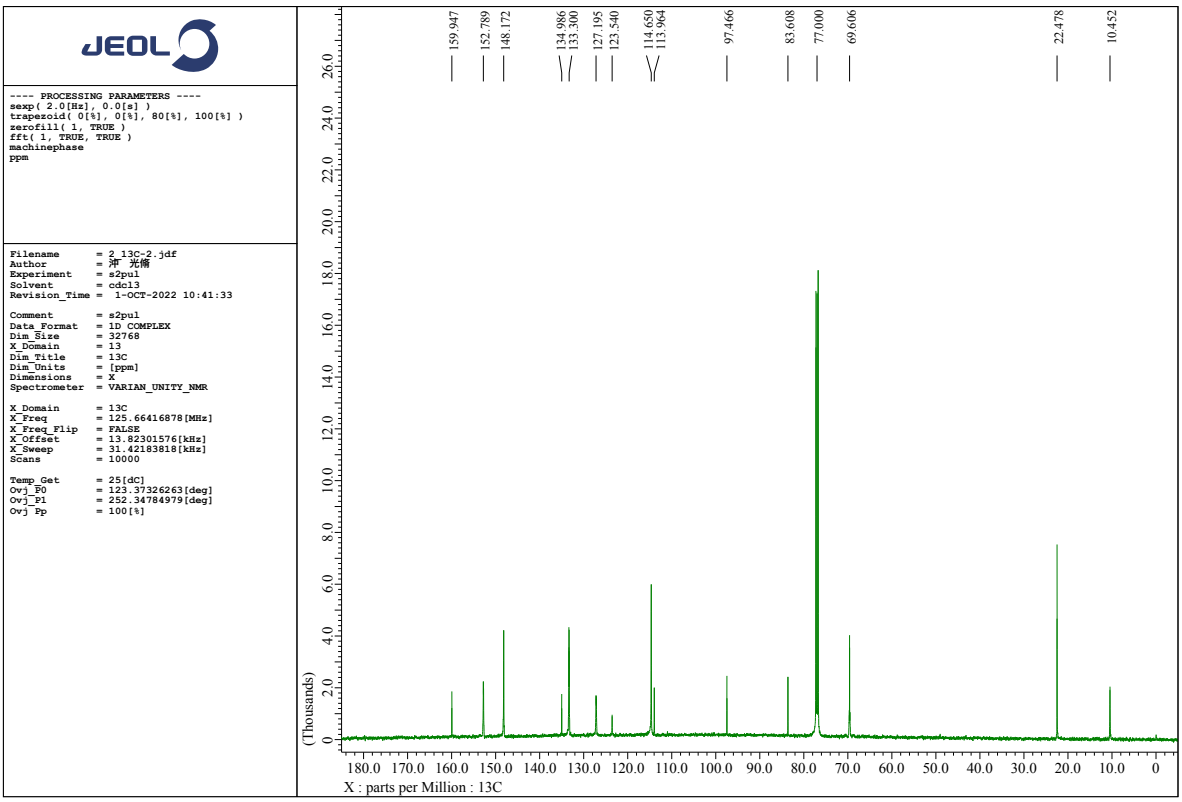

Fig. S11. ^{13}C NMR (126 MHz, $CDCl_3$, 25 °C) spectrum of **5**.

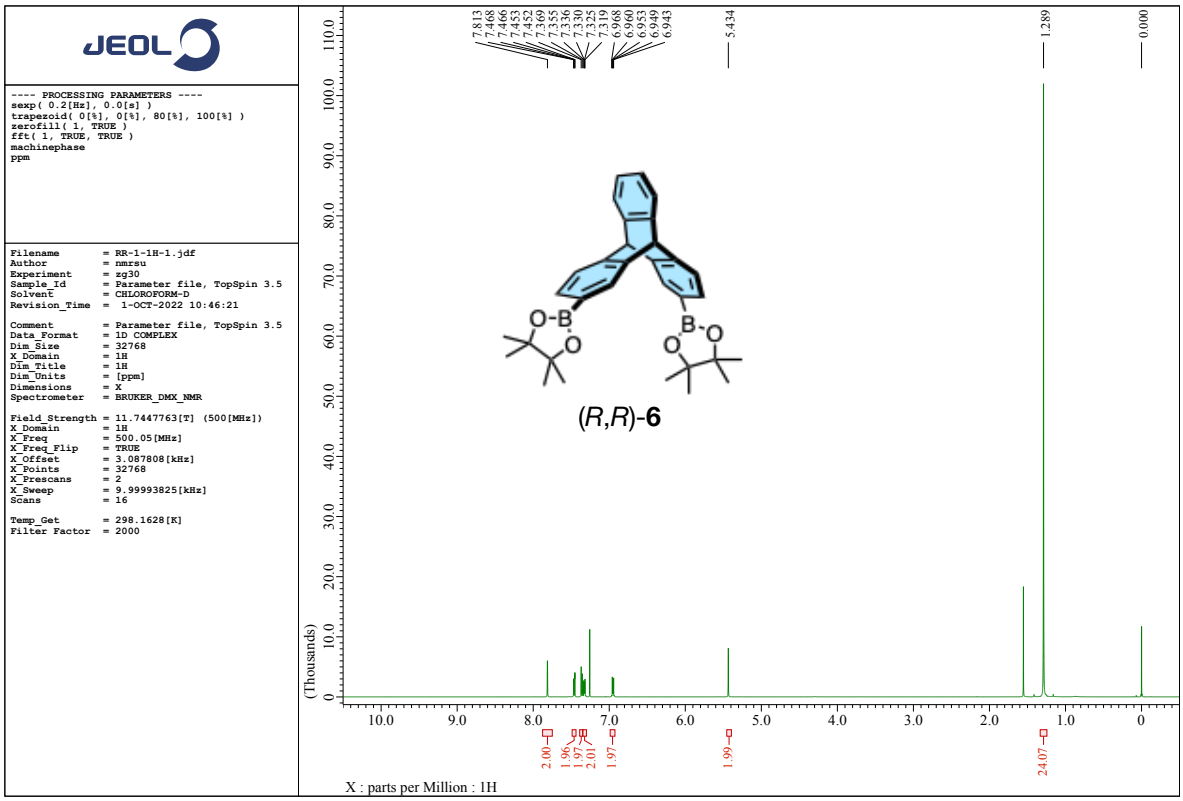

Fig. S12. ^{1}H NMR (500 MHz, $CDCl_3$, rt) spectrum of (*R*,*R*)-**6**.

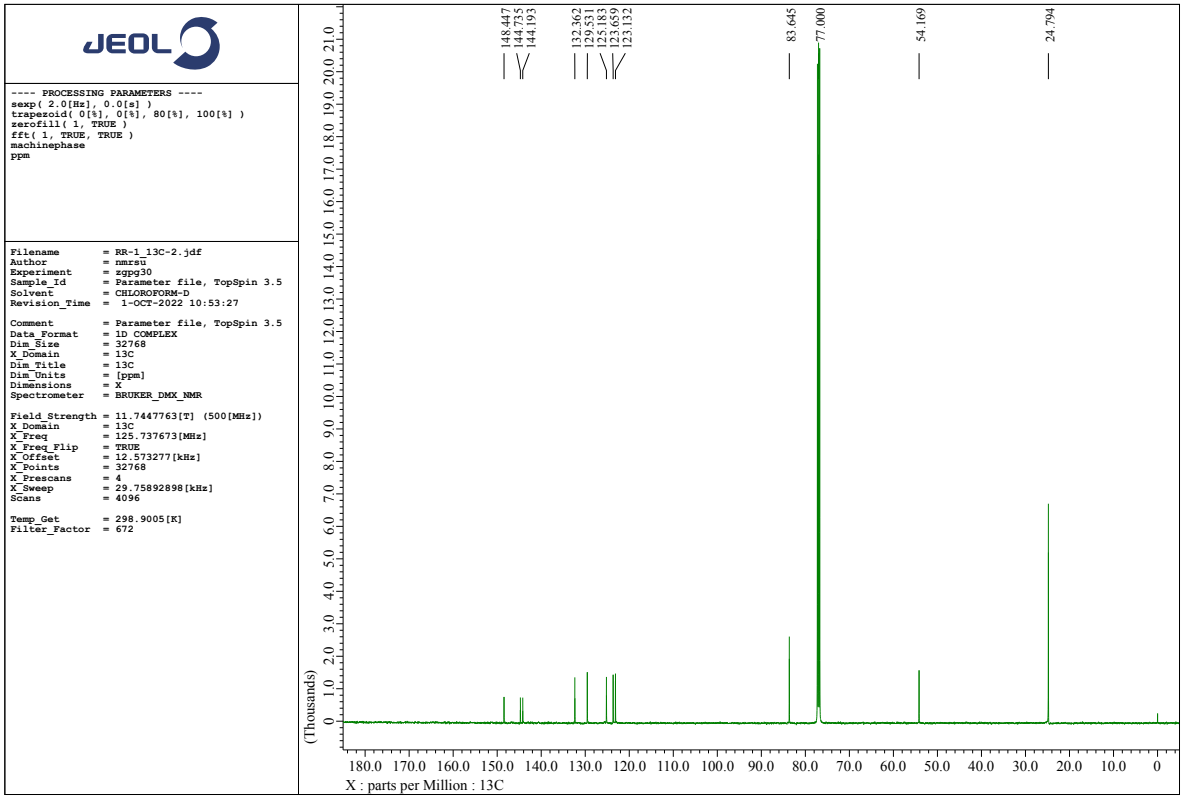

Fig. S13. ^{13}C NMR (126 MHz, $CDCl_3$, rt) spectrum of (*R*,*R*)-**6**.

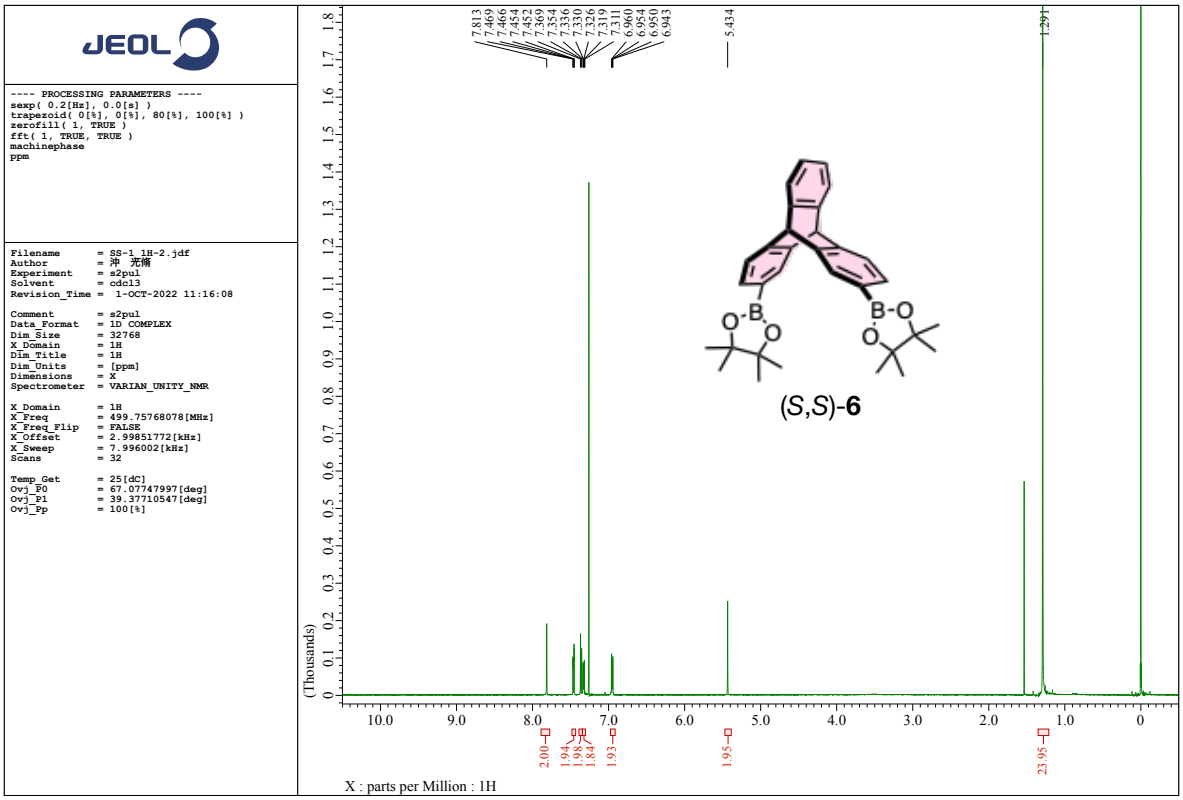

Fig. S14. ^{1}H NMR (500 MHz, $CDCl_3$, 25 °C) spectrum of (*S*,*S*)-**6**.

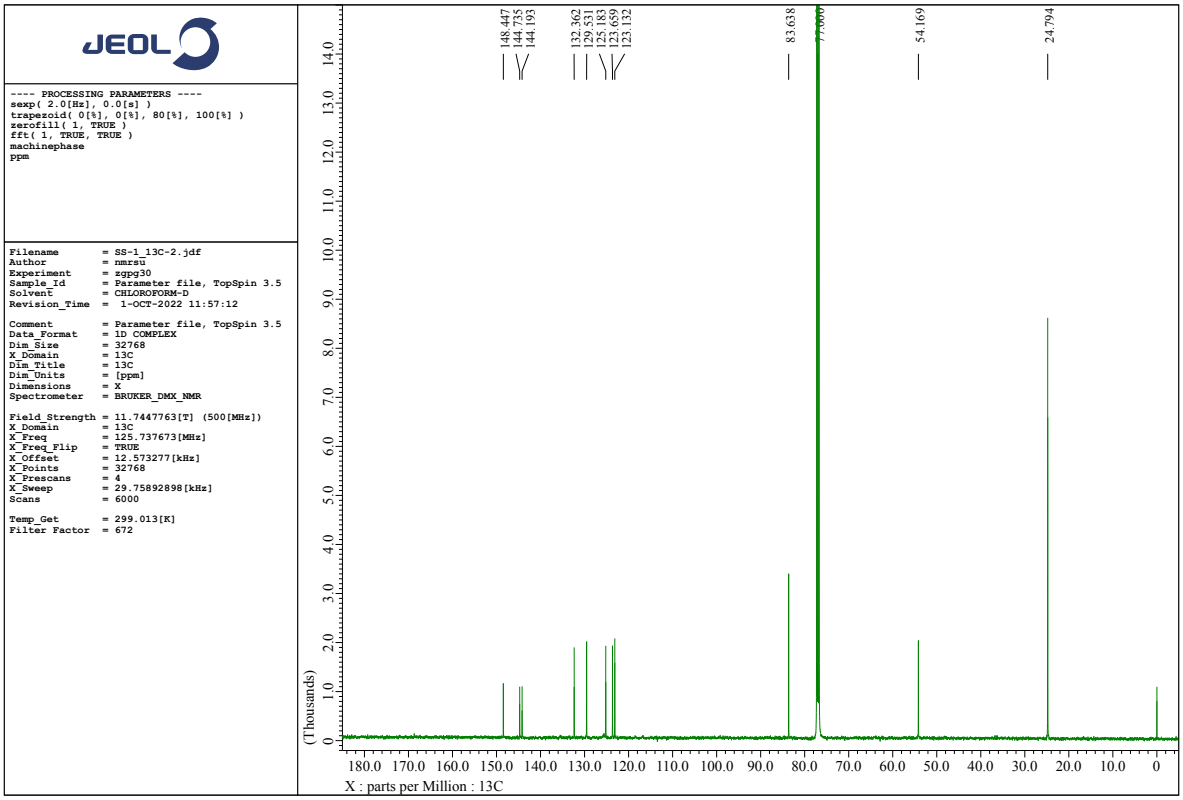

Fig. S15. ^{13}C NMR (126 MHz, $CDCl_3$, rt) spectrum of (*S*,*S*)-**6**.

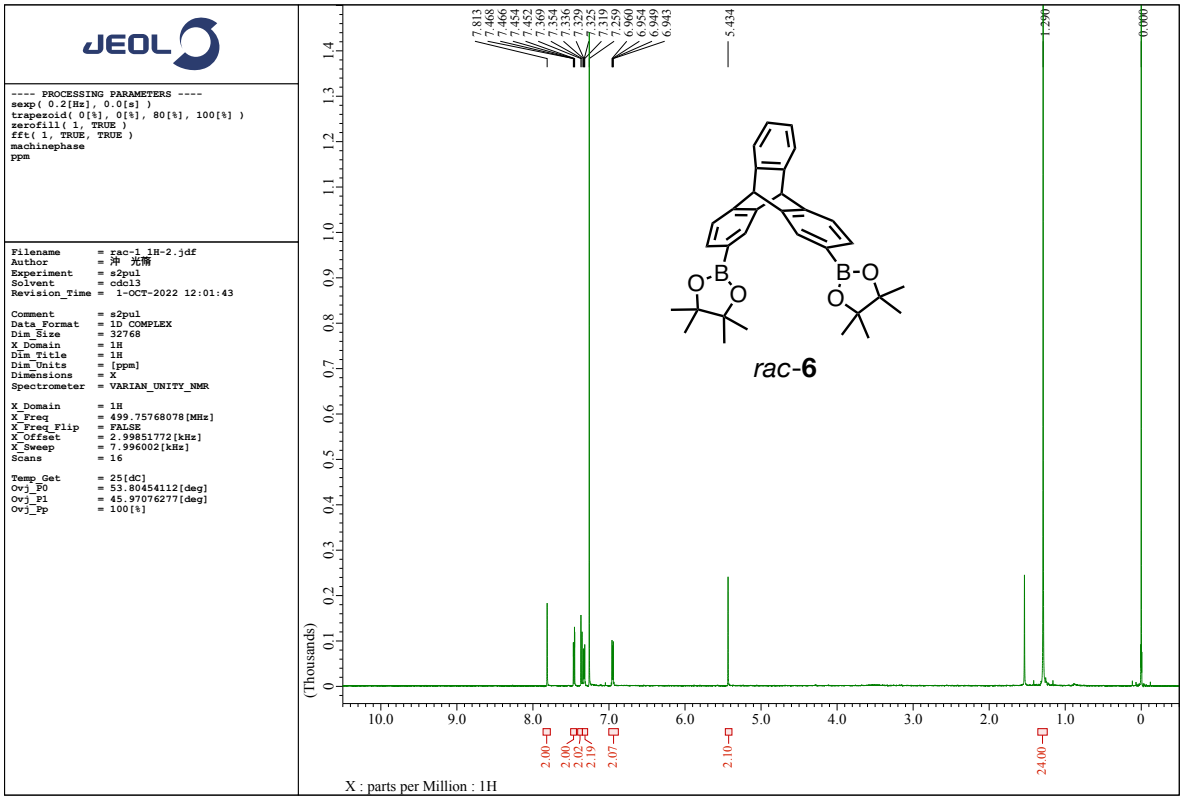

Fig. S16. ^{1}H NMR (500 MHz, $CDCl_3$, 25 °C) spectrum of *rac*-**6**.

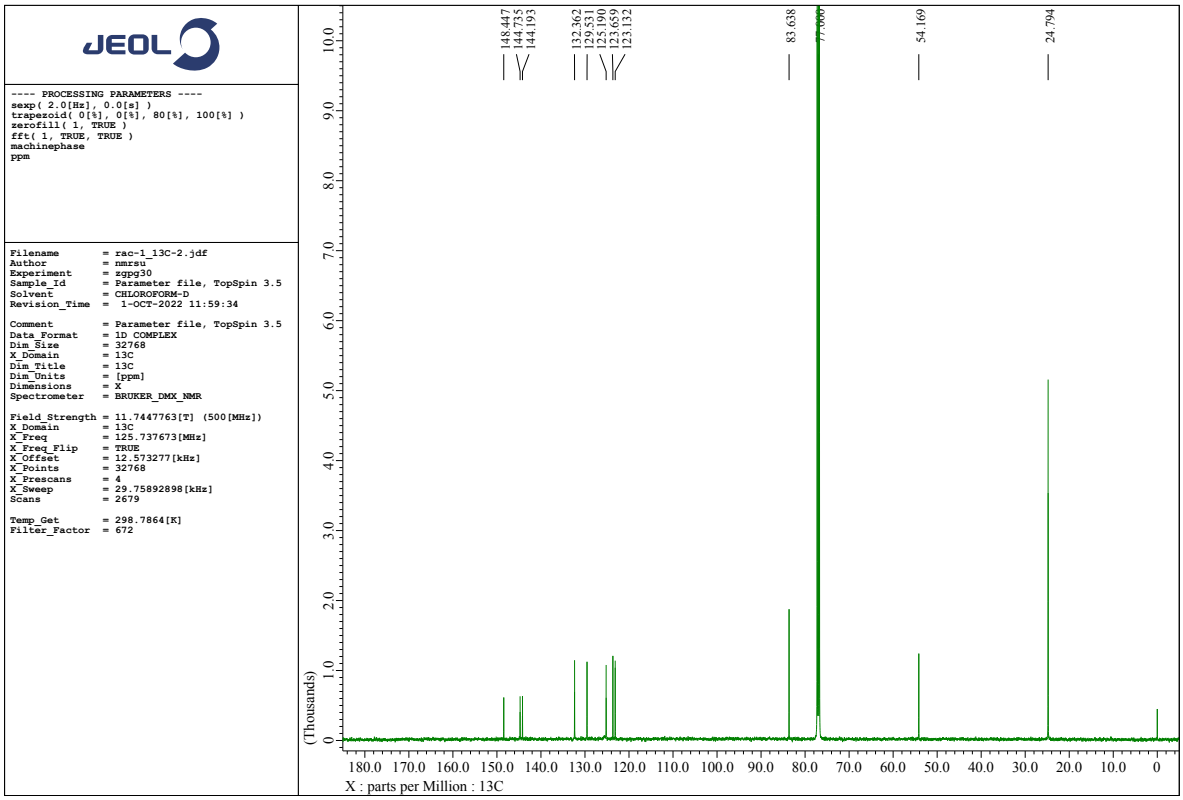

Fig. S17. ^{13}C NMR (126 MHz, $CDCl_3$, rt) spectrum of *rac*-**6**.

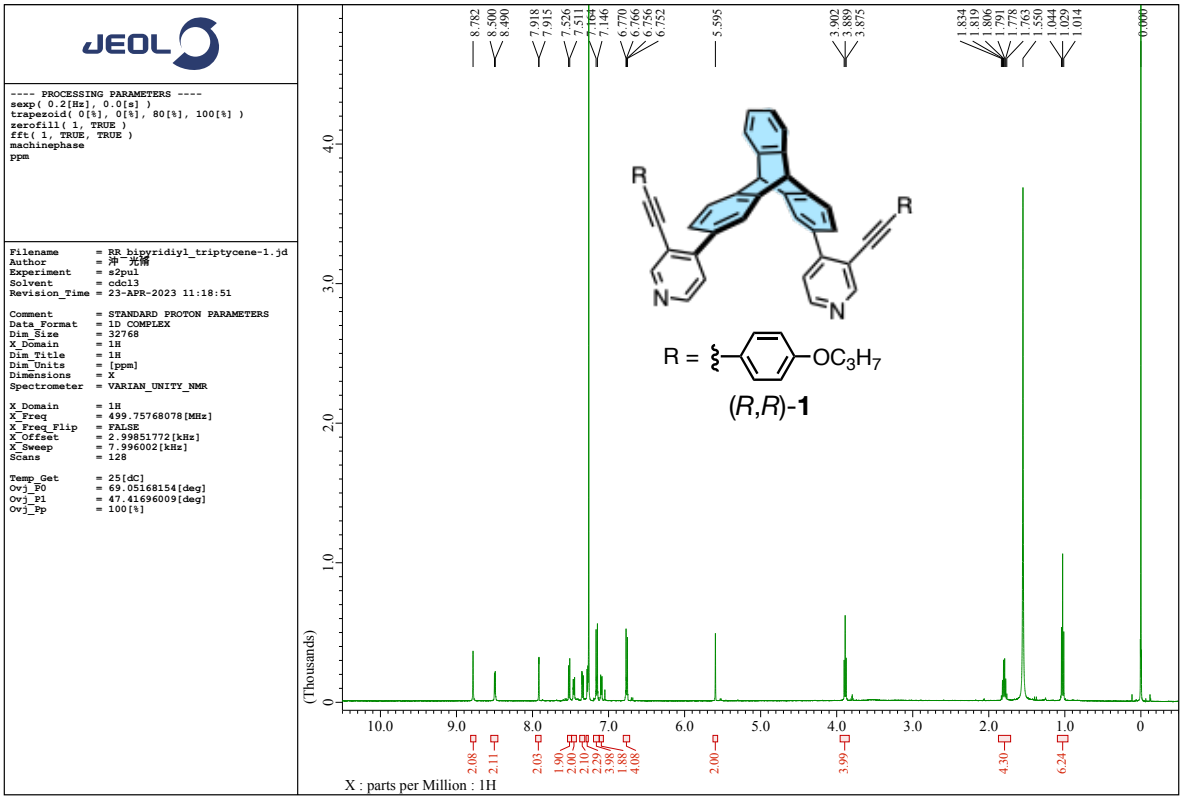

Fig. S18. ^{1}H NMR (500 MHz, $CDCl_3$, 25 °C) spectrum of (*R*,*R*)-**1**.

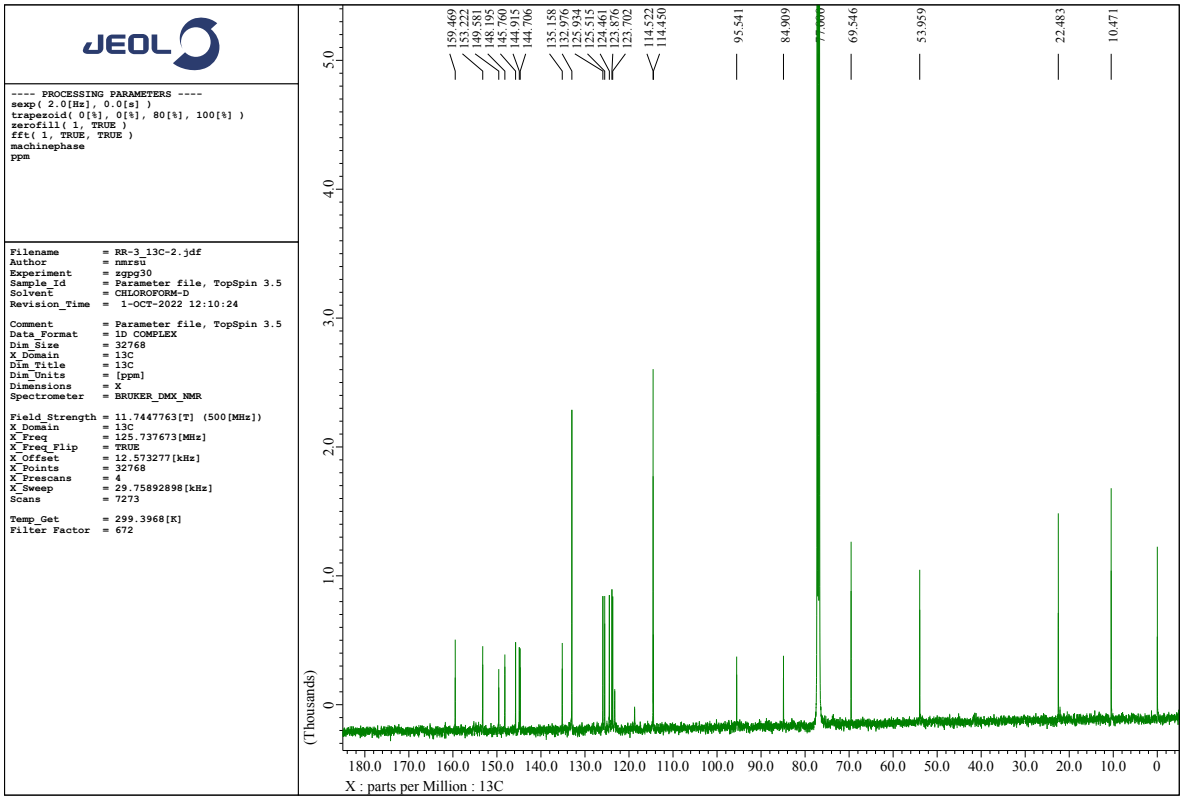

Fig. S19. ^{13}C NMR (126 MHz, $CDCl_3$, rt) spectrum of (*R*,*R*)-**1**.

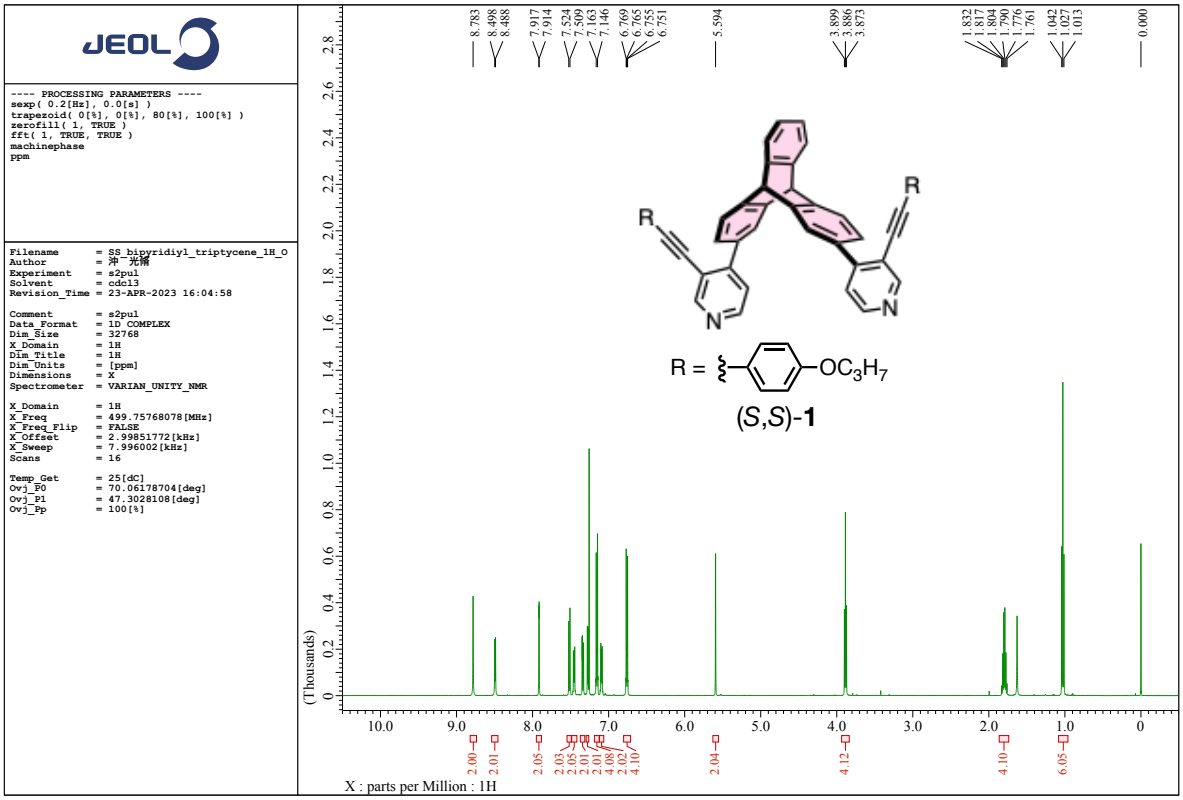

Fig. S20. ^{1}H NMR (500 MHz, $CDCl_3$, 25 °C) spectrum of (*S*,*S*)-**1**.

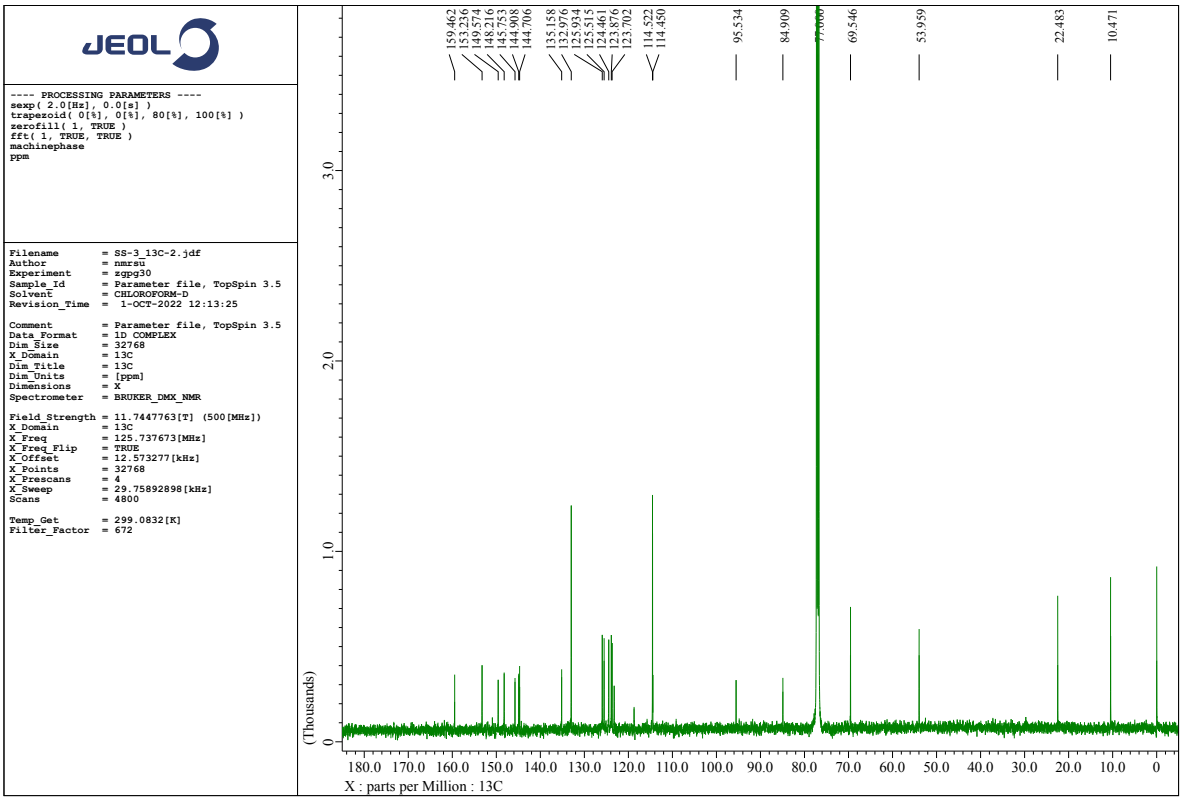

Fig. S21. ^{13}C NMR (126 MHz, $CDCl_3$, rt) spectrum of (*S*,*S*)-**1**.

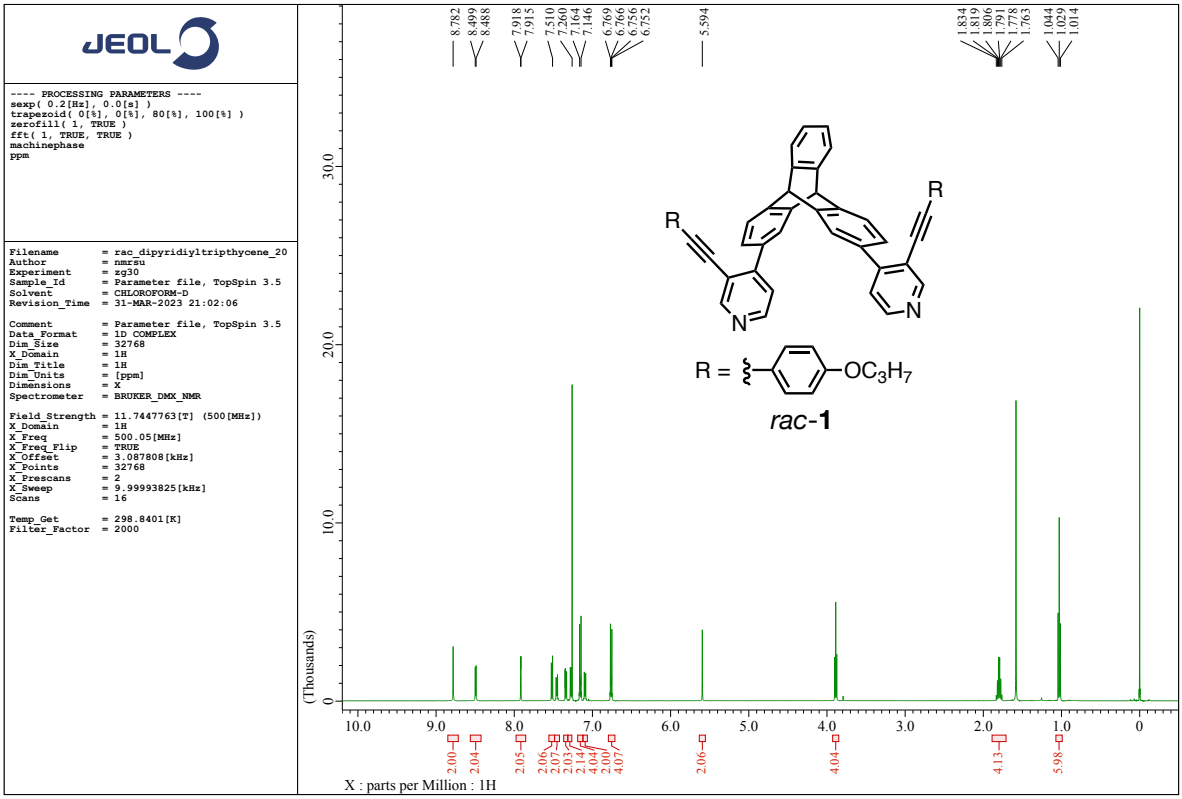

Fig. S22. ^{1}H NMR (500 MHz, $CDCl_3$, rt) spectrum of *rac*-**1**.

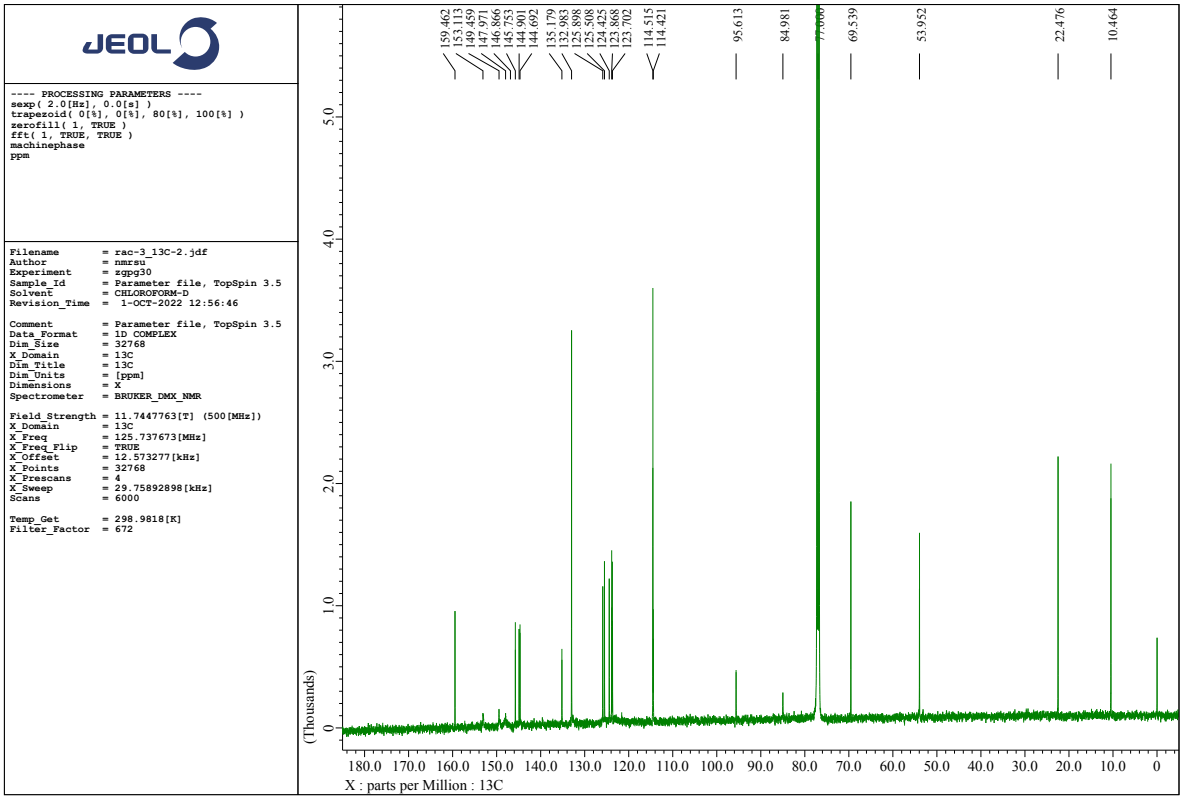

Fig. S23. ^{13}C NMR (126 MHz, $CDCl_3$, rt) spectrum of *rac*-**1**.

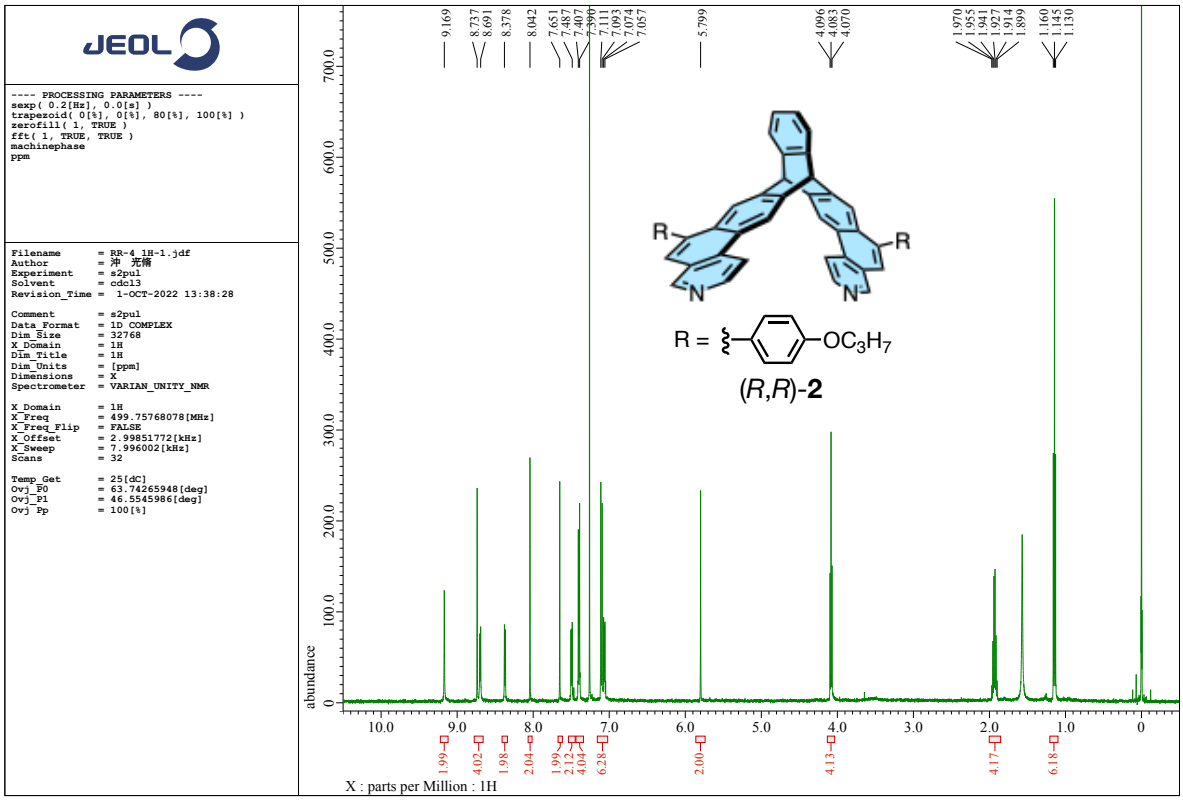

Fig. S24. ^{1}H NMR (500 MHz, $CDCl_3$, 25 °C) spectrum of (*R*,*R*)-**2**.

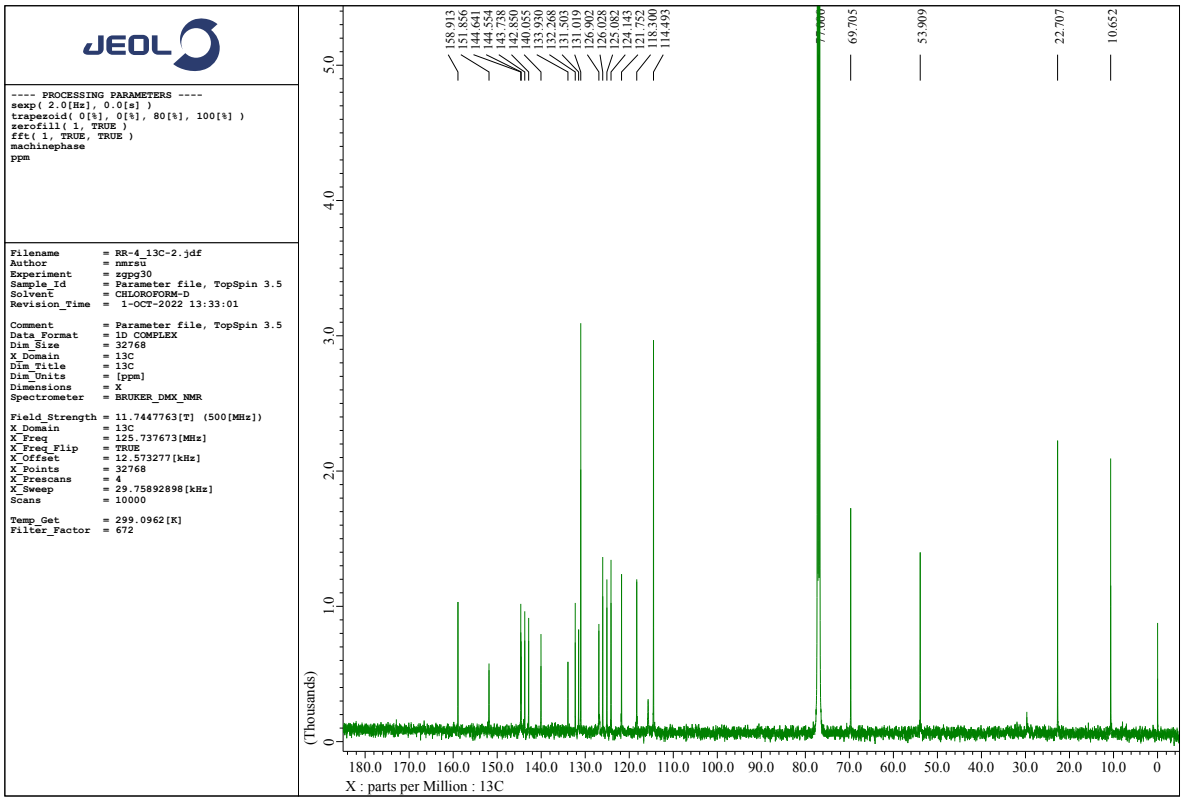

Fig. S25. ^{13}C NMR (126 MHz, $CDCl_3$, rt) spectrum of (*R*,*R*)-**2**.

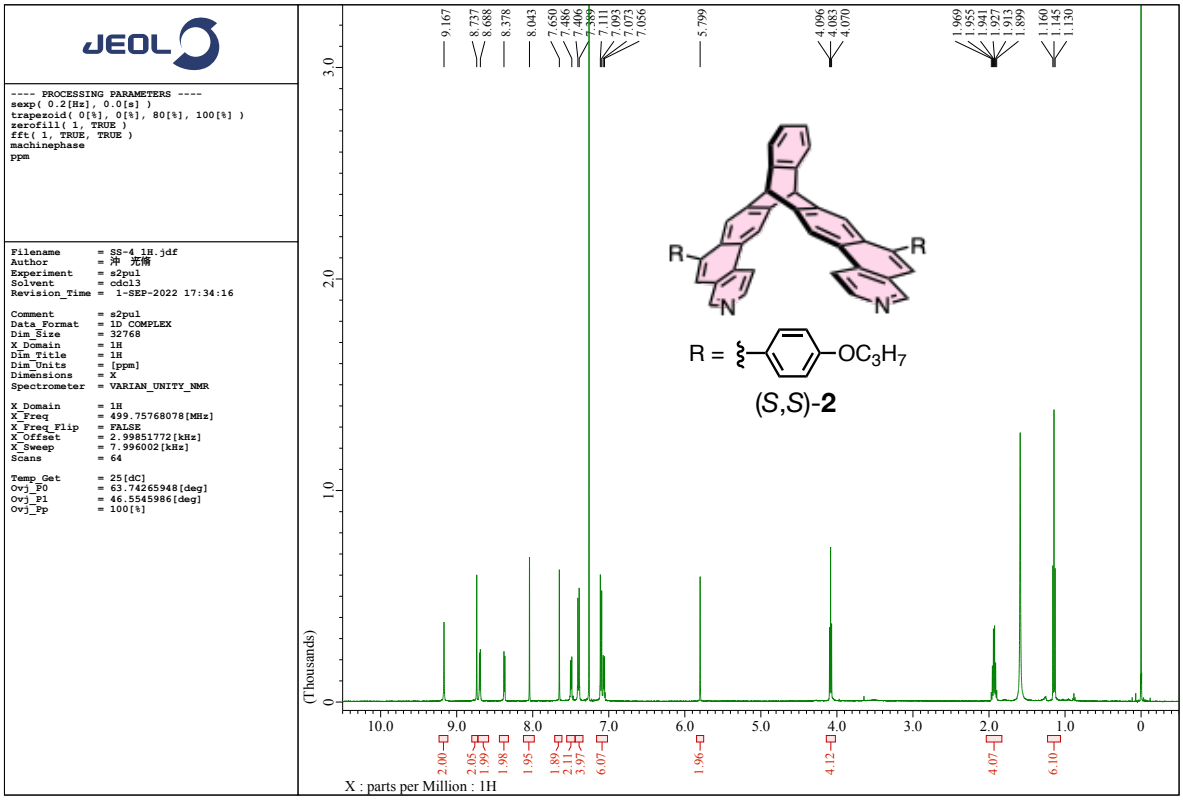

Fig. S26. ^{1}H NMR (500 MHz, $CDCl_3$, 25 °C) spectrum of (*S*,*S*)-**2**.

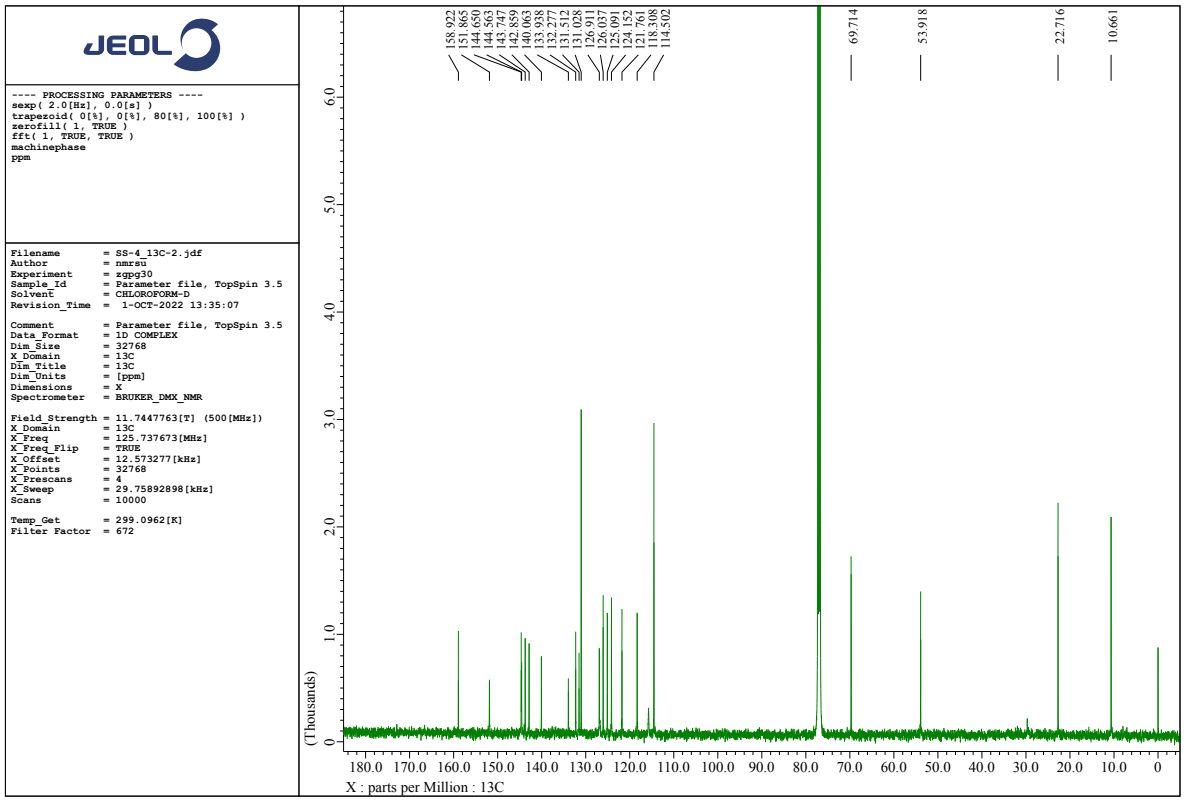

Fig. S27. ^{13}C NMR (126 MHz, $CDCl_3$, rt) spectrum of (*S*,*S*)-**2**.

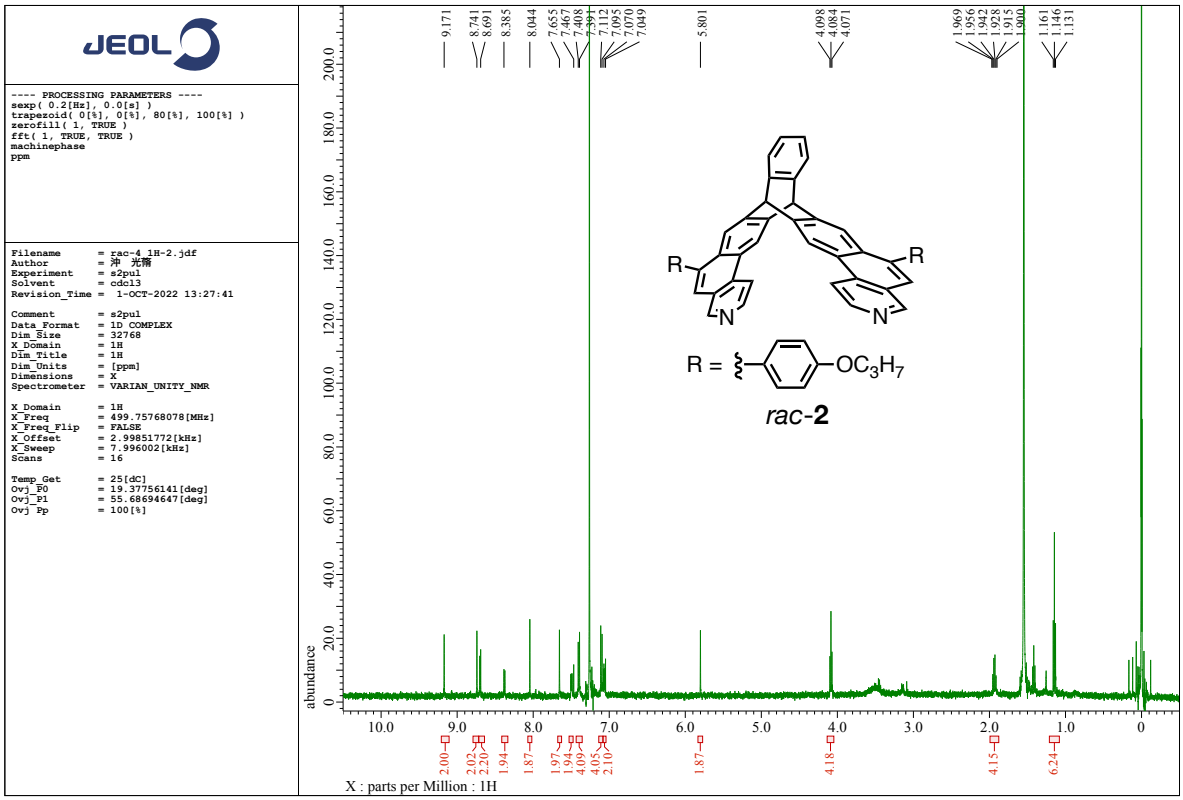

Fig. S28. ^{1}H NMR (500 MHz, $CDCl_3$, 25 °C) spectrum of *rac*-**2**.

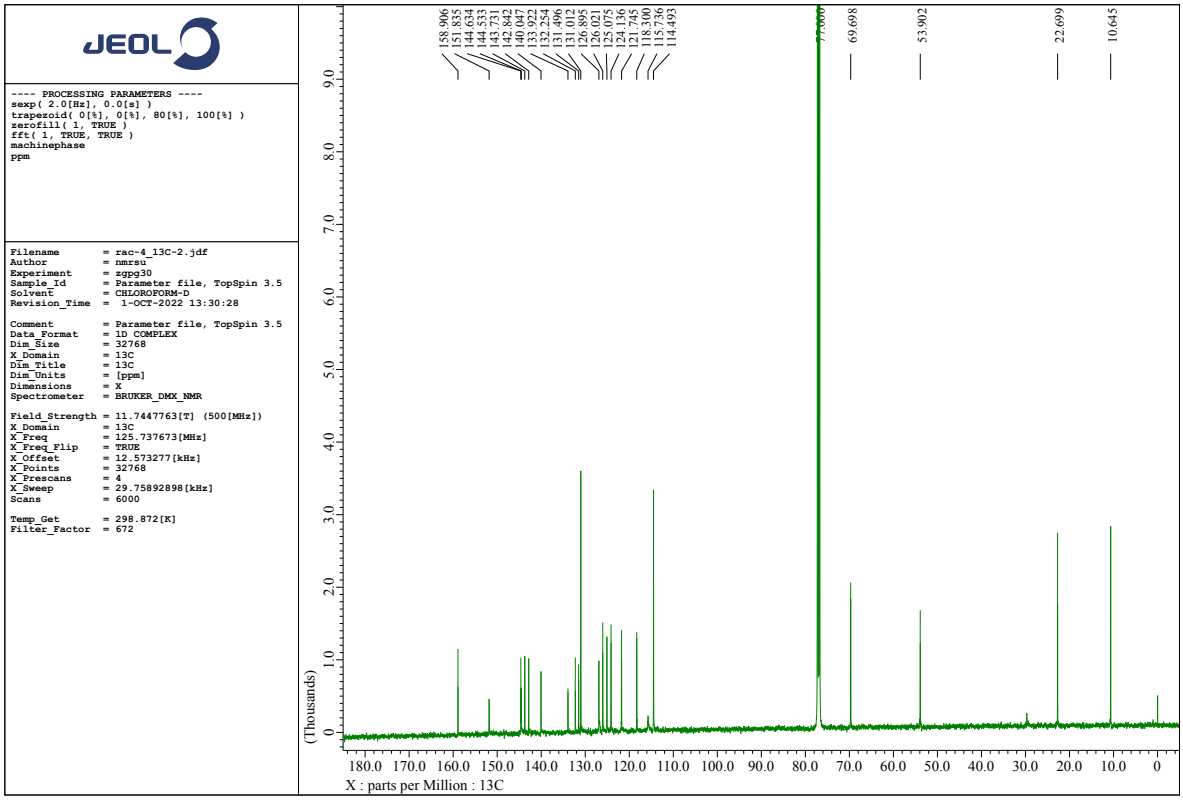

Fig. S29. ^{13}C NMR (126 MHz, $CDCl_3$, rt) spectrum of *rac*-**2**.

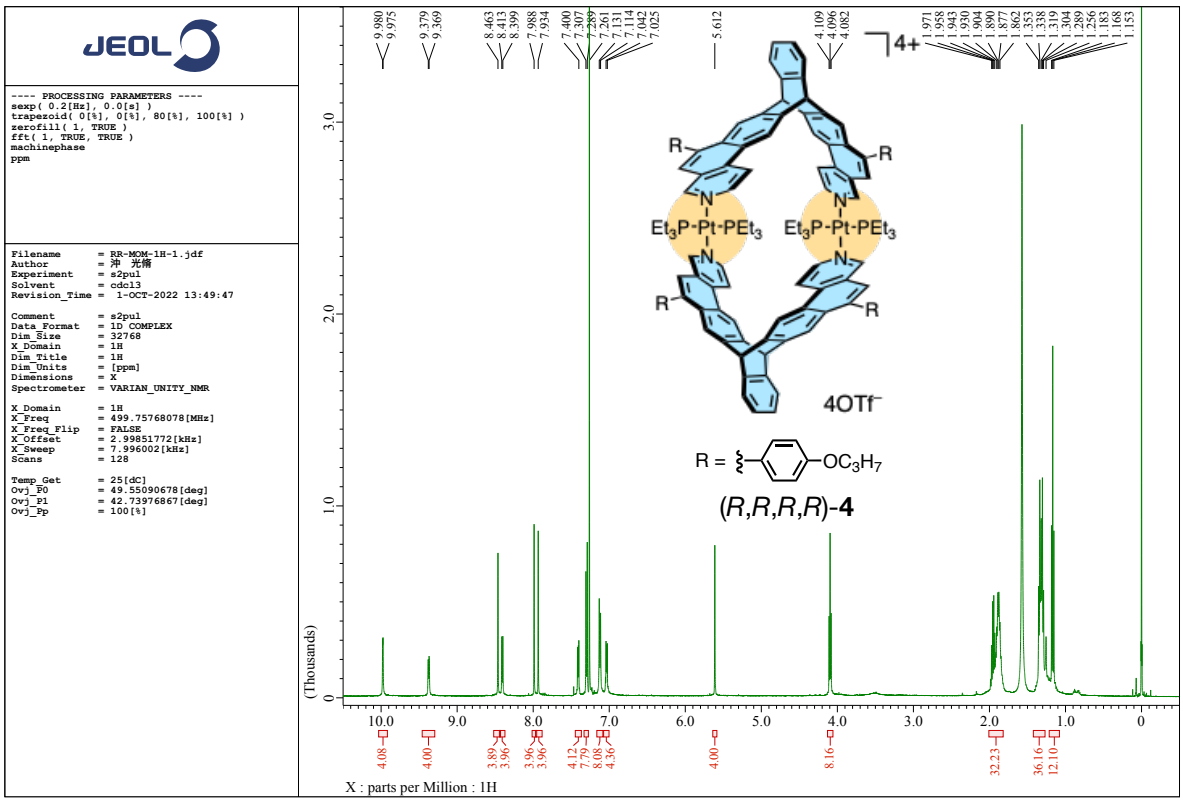

Fig. S30. ^{1}H NMR (500 MHz, $CDCl_3$, 25 °C) spectrum of (*R*,*R*,*R*,*R*)-**4**.

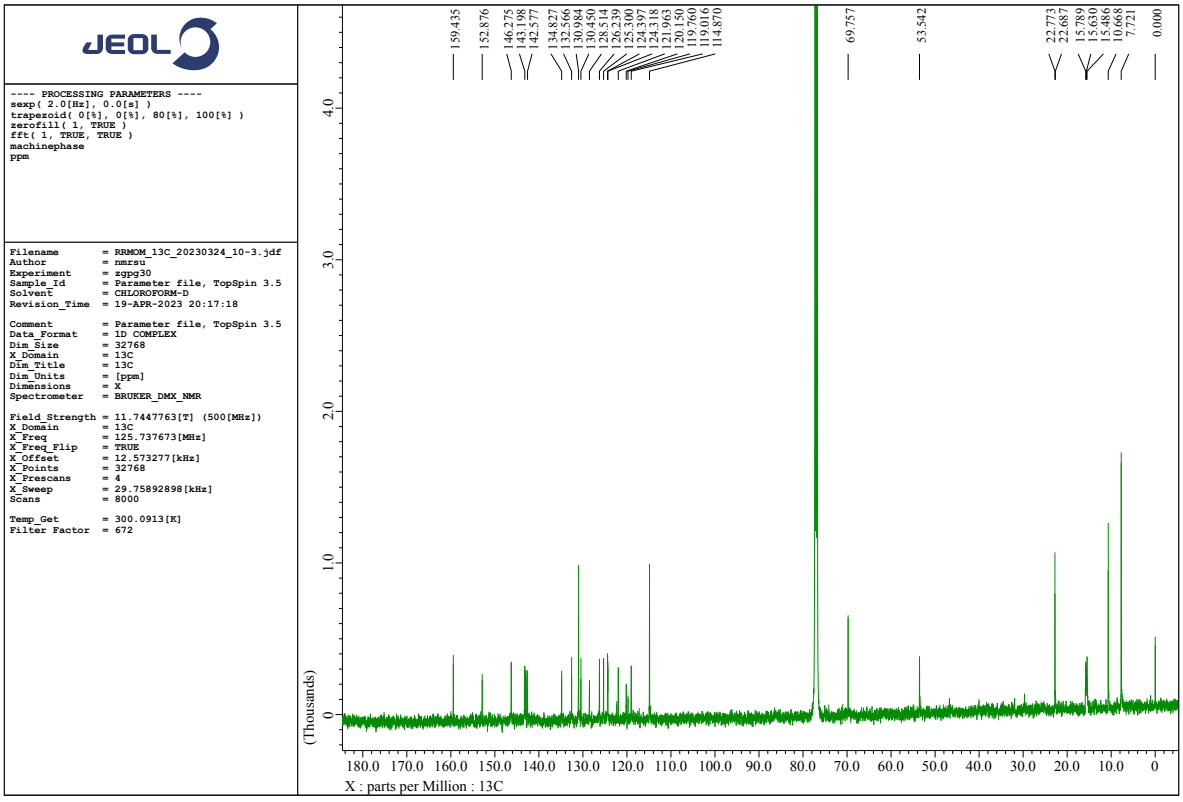

Fig. S31. ^{13}C NMR (126 MHz, $CDCl_3$, rt) spectrum of (*R*,*R*,*R*,*R*)-**4**.

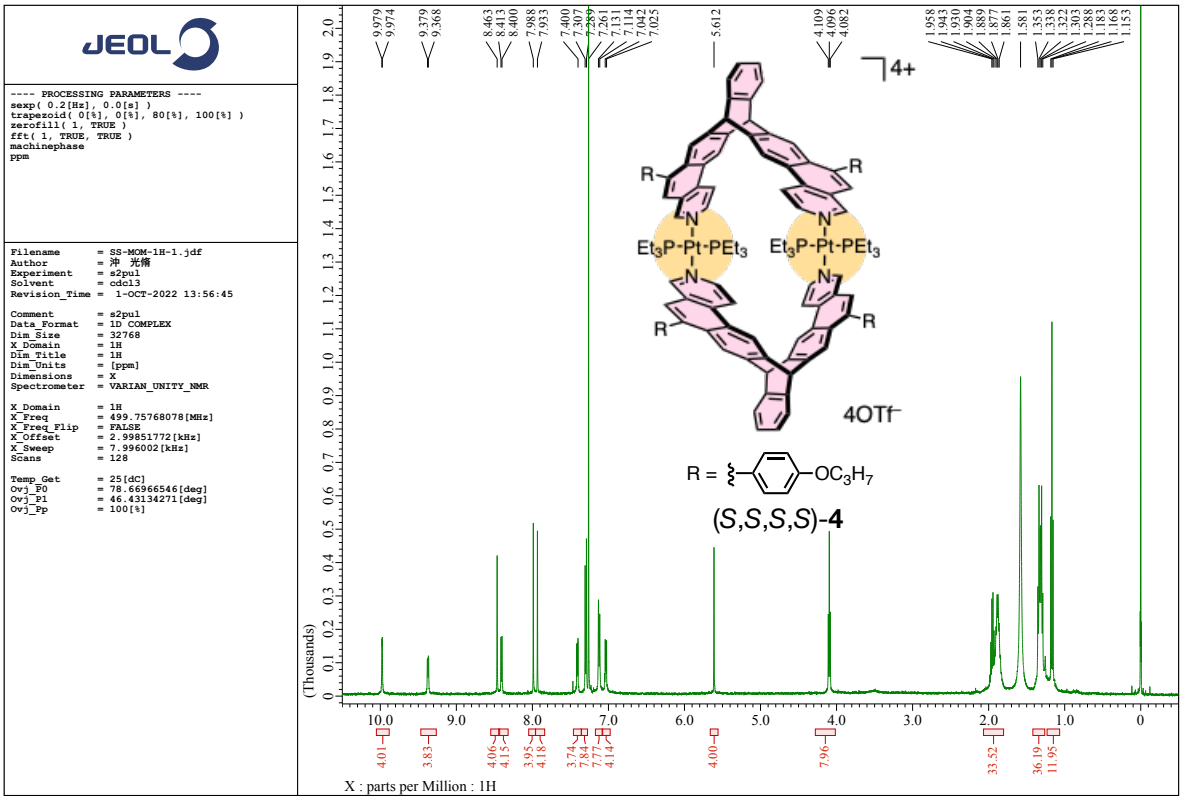

Fig. S32. ^{1}H NMR (500 MHz, $CDCl_3$, 25 °C) spectrum of (*S*,*S*,*S*,*S*)-**4**.

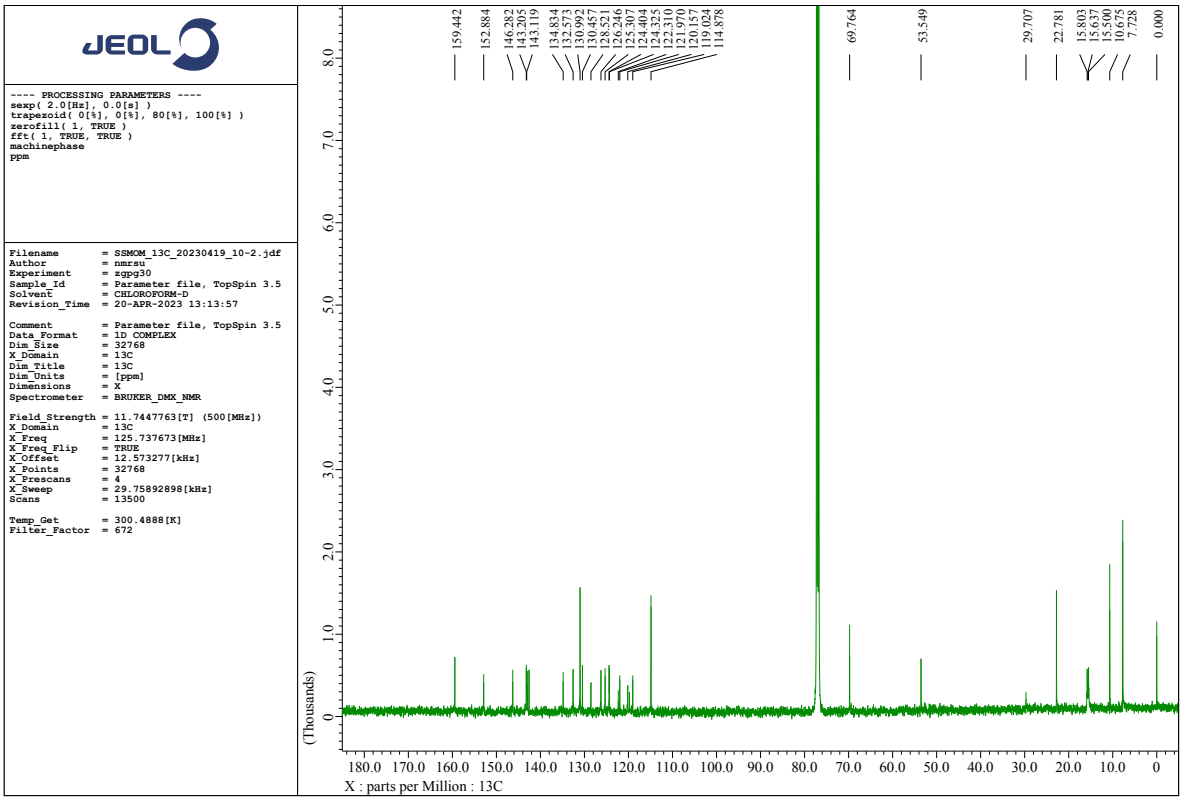

Fig. S33. ^{13}C NMR (126 MHz, $CDCl_3$, rt) spectrum of (*S*,*S*,*S*,*S*)-**4**.

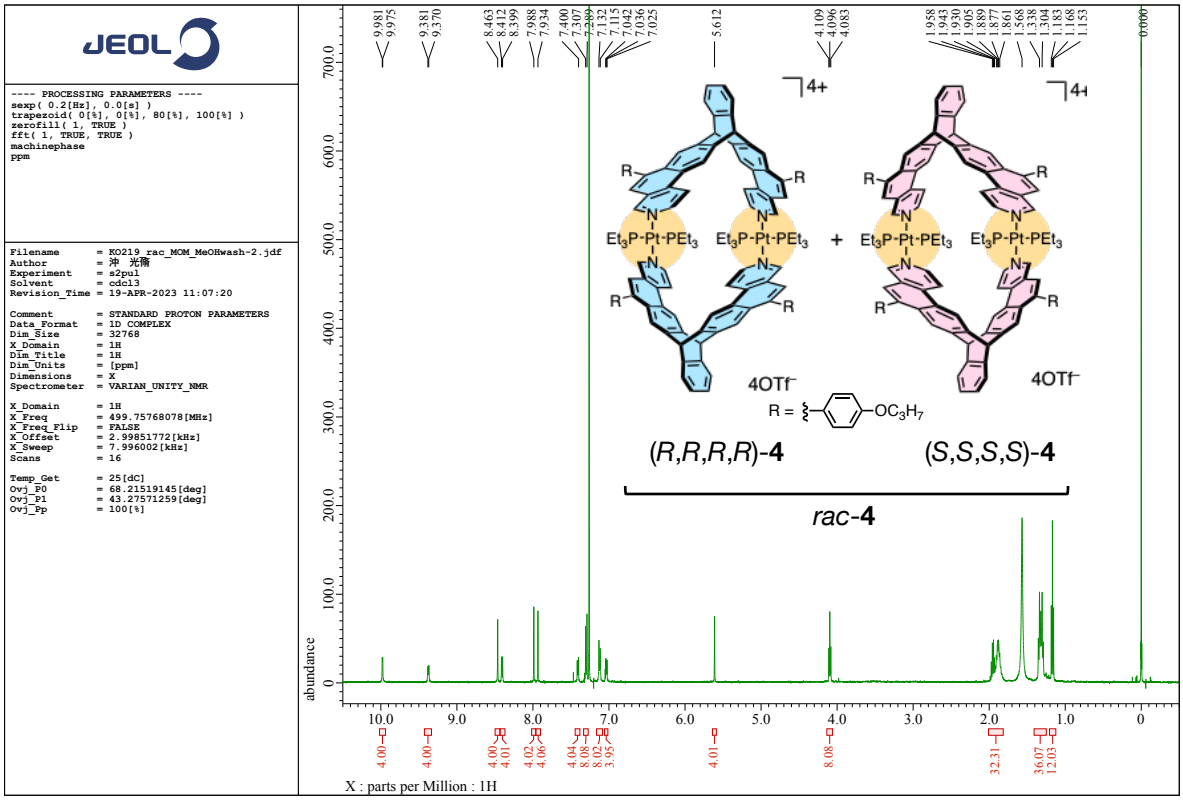

Fig. S34. ^{1}H NMR (500 MHz, $CDCl_3$, 25 °C) spectrum of *rac*-**4**.

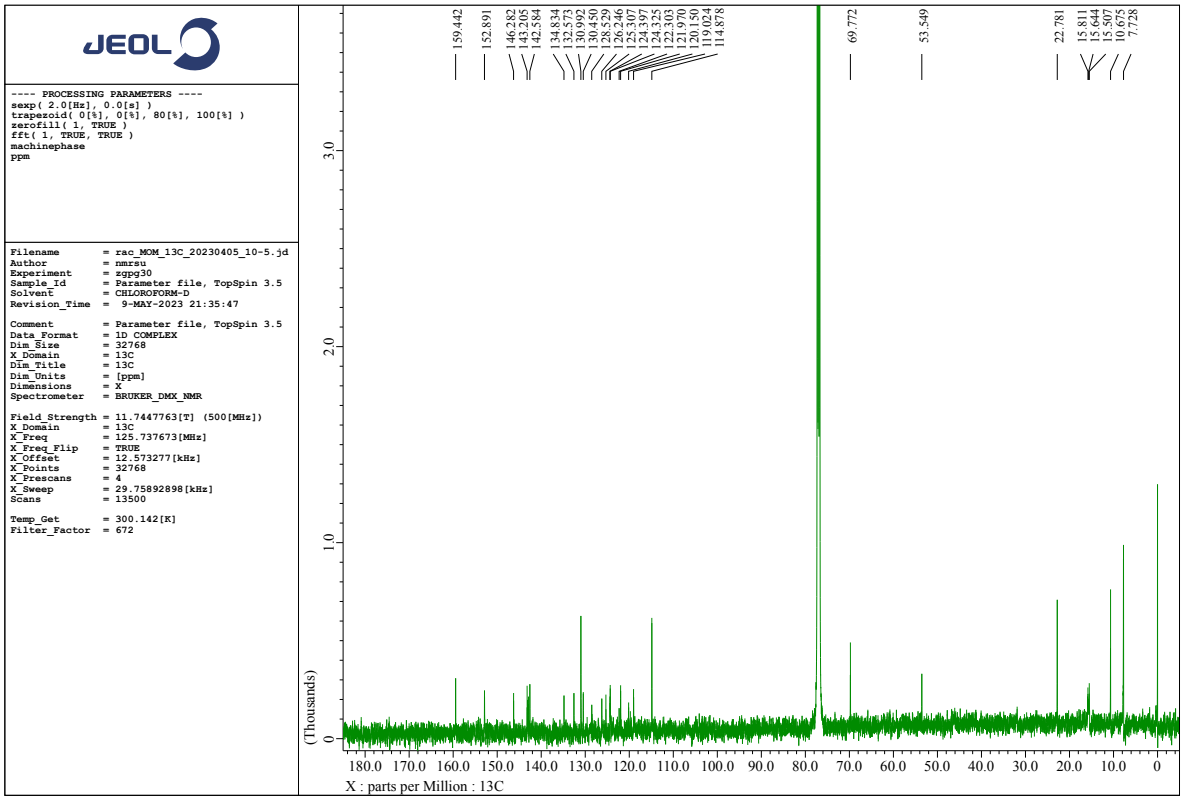

Fig. S35. ^{13}C NMR (126 MHz, $CDCl_3$, rt) spectrum of *rac*-**4**.